



Since January 2020 Elsevier has created a COVID-19 resource centre with free information in English and Mandarin on the novel coronavirus COVID-19. The COVID-19 resource centre is hosted on Elsevier Connect, the company's public news and information website.

Elsevier hereby grants permission to make all its COVID-19-related research that is available on the COVID-19 resource centre - including this research content - immediately available in PubMed Central and other publicly funded repositories, such as the WHO COVID database with rights for unrestricted research re-use and analyses in any form or by any means with acknowledgement of the original source. These permissions are granted for free by Elsevier for as long as the COVID-19 resource centre remains active.



Research paper

Discovery, synthesis, and optimization of an *N*-alkoxy indolylacetamide against HIV-1 carrying NNRTI-resistant mutations from the *Isatis indigotica* root

Chengbo Xu ^{a,1}, Yijing Xin ^{a,1}, Minghua Chen ^{a,b}, Mingyu Ba ^a, Qinglan Guo ^a,
Chenggen Zhu ^a, Ying Guo ^{a,**}, Jiangong Shi ^{a,*}

^a State Key Laboratory of Bioactive Substance and Function of Natural Medicines, Institute of Materia Medica, Chinese Academy of Medical Sciences and Peking Union Medical College, Beijing, 100050, China

^b Institute of Medicinal Biotechnology, Chinese Academy of Medical Sciences and Peking Union Medical College, Beijing, 100050, China

ARTICLE INFO

Article history:

Received 9 November 2019

Received in revised form

4 January 2020

Accepted 13 January 2020

Available online 22 January 2020

Keywords:

Isatis indigotica

N-Alkyloxy indole derivative

HIV-1 inhibitor

Derivative synthesis

Structure-activity relationship

NNRTI

ABSTRACT

From an aqueous decoction of the traditional Chinese medicine “ban lan gen” (the *Isatis indigotica* root), an antiviral natural product **CI - 39** was isolated as an NNRTI (non-nucleoside reverse transcriptase inhibitor) ($EC_{50} = 3.40 \mu\text{M}$). Its novel structure was determined as methyl (1-methoxy-1*H*-indol-3-yl) acetamidobenzoate by spectroscopic data and confirmed by single crystal X-ray diffraction. Through synthesis and structure-activity relationship (SAR) investigation of **CI - 39** and 57 new derivatives (24 with EC_{50} values of 0.06–8.55 μM), two optimized derivatives **10f** and **10i** (EC_{50} : 0.06 μM and 0.06 μM) having activity comparable to that of NVP ($EC_{50} = 0.03 \mu\text{M}$) were obtained. Further evaluation verified that **10f** and **10i** were RT DNA polymerase inhibitors and exhibited better activities and drug resistance folds compared to NVP against seven NNRTI-resistant strains carrying different mutations. Especially, **10i** ($EC_{50} = 0.43 \mu\text{M}$) was more active to the L100I/K103N double-mutant strain as compared to both NVP ($EC_{50} = 0.76 \mu\text{M}$) and EFV ($EC_{50} = 1.08 \mu\text{M}$). The molecular docking demonstrated a possible binding pattern between **10i** and RT and revealed activity mechanism of **10i** against the NNRTI-resistant strains.

© 2020 Elsevier Masson SAS. All rights reserved.

1. Introduction

Acquired immunodeficiency syndrome (AIDS) is caused by the human immunodeficiency virus (HIV) infection, which destroys the body's immune system by infecting human immune cells and causing patients to eventually die from complications such as severe infections or secondary tumors [1,2]. In 2018, there were approximately 37.9 million people worldwide living with HIV/AIDS, including 1.7 million children [3]. Moreover, 1.7 million individuals became newly infected in 2018. As there is no AIDS vaccine available, highly active antiretroviral therapy (HAART) is still the main clinical treatment of HIV/AIDS. Many HAART comprises two or three antiretroviral drugs acting on different targets, such as reverse transcriptase (RT), protease (PR), and integrase (IN) [4–6].

However, long-term widespread use of HAART can lead to drug-resistant viruses and treatment failure [7]. At least 50% of patients have drug-resistant viruses. The non-nucleoside reverse transcriptase inhibitors (NNRTIs) nevirapine (NVP) and efavirenz (EFV) have been used for more than 10 years in clinical practice, and stable drug-resistant strains have emerged [8]. Clinical studies have found that after 48 weeks of etravirine and rilpivirine administration, the body produces a virus resistant to both the drugs. Several new forms of NNRTIs have been reported in recent years [9–16]. In consideration of drug resistance continues to increase, the development of new NNRTIs is still worth the challenge.

“Ban lan gen” (*Isatis indigotica* root) is one of the most important traditional Chinese medicines used for the treatment of influenza and various infectious diseases [17] as well as anti-severe acute respiratory syndrome (SARS) [18]. Previous studies demonstrated that indirubin, one of the bioactive indole alkaloids of the herbal drug, had the most significant cytotoxicity on IL-60 cells and inhibitory effect on pseudorabies virus (PrV) replication, while extracts from roots and leaves of *I. indigotica* also showed

* Corresponding author.

** Corresponding author.

E-mail addresses: yingguo6@imm.ac.cn (Y. Guo), shijg@imm.ac.cn (J. Shi).

¹ These authors contributed equally.

cytopathic effect (CPE) reduction either before or after infection of PrV on porcine kidney (PK-15) cells [18]. Moreover, from the ethanol extract of “da qing ye” (*I. indigotica* leaves) an isatisine A-derived artificial acetamide was reported to have a moderate anti-HIV-1 activity ($EC_{50} = 37.8 \mu\text{M}$) [19]. However as far as we know, was neither extract or purified compound from “ban lan gen” reported to inhibit HIV virus replication. Because the “ban lan gen” decoction is practically used in clinic, whereas the ethanolic extracts were mainly focused in the previous studies, we systematically studied the chemical constituents and biological activities of an aqueous extract of the *I. indigotica* root, resulted in characterization of more than 100 chemical constituents including around 50 alkaloids and some with antiviral (influenza virus A/Hanfng/359/95, herpes simplex virus 1, and/or Coxsackie virus B3) and cell-damage protective activities [20–34]. A continuation of the work led to characterization of a novel anti-HIV compound methyl (1-methoxy-1*H*-indol-3-yl)acetamidobenzoate (**CI - 39**) (Fig. 1A) with an EC_{50} value of $3.40 \mu\text{M}$ from a remaining subfraction. **CI - 39** represents the first anti-HIV-1 indolylacetamidobenzoate derivative from *I. indigotica*, though from other plants a variety of natural products and extracts with inhibition of HIV-1 replication were reported [35–40].

In view of the structure of **CI - 39** and its inhibitory effect on the HIV-1 virus, along with the recent reports on indole derivatives with anti-HIV activity [41–55], we determined that the optimization of activity and physicochemical properties by synthesis to obtain optimized lead compounds or drug candidates was worthy of further study. Because of limitation of the sample amount from the plant extract, **CI - 39** was firstly synthesized with confirmation of the anti-HIV-1 replication. For the structural optimization, the effect of the following structural changes on the anti-HIV-1 activity were investigated in this study: (i) the shift of methoxyformyl on the phenylamine moiety with replacement or introduction of other functional groups; (ii) the replacement of the phenyl ring with an aromatic heterocyclic ring; (iii) the substitution of the *N*-methoxy group on the indole nucleus by other *N*-alkoxy groups; (iv) the extension or shortening of the acetamide linker between the indole and phenyl ring units. The synthetic lead compound **CI - 39** and most potent derivatives were further tested for their activity against the HIV-1 strains carrying some of the most clinically relevant mutations that confer resistance to NNRTIs. Herein, reported are isolation, structural determination, and synthesis of the lead compound **CI - 39**, along with synthesis, anti-HIV-1 activity, and structure-activity relationship of 57 new derivatives as well as activity of three optimized compounds **6d**, **10f**, and **10i** as novel NNRTIs against seven NNRTI-resistant HIV-1 strains carrying different RT-mutations. Molecular docking of the lead compound **CI - 39** and the most potent compound **10i** is also discussed.

2. Results and discussion

2.1. Chemistry

2.1.1. Isolation, structure elucidation, and antiviral assay of **CI - 39**

The aqueous decoction of the air-dried and pulverized *I. indigotica* root was concentrated under reduced pressure and separated by column chromatography (CC) over macroporous adsorbent resin (HPD-110), eluting successively with H_2O , 50% EtOH, and 95% EtOH, to yield three corresponding fractions A, B and C. Fraction C was subjected to CC over silica gel, with elution using a gradient of increasing acetone concentration (0–100%) in petroleum ether, to afford fractions C1–C11 [20]. Fraction C9 was separated successively by CC over Sephadex LH-20, reversed phase silica gel (C_{18}), and silica gel to give a mixture, from which **CI - 39** was isolated by HPLC using a semipreparative C_{18} column (see Experimental section 4.1.1).

Compound **CI - 39** was obtained as colorless prisms in acetone. Its IR spectrum showed the presence of amino (3247 cm^{-1}), ester and amide carbonyl (1701 and 1677 cm^{-1}), and aromatic ring (1585 and 1511 cm^{-1}) functionalities in the molecule. Combinatory analysis of HRMS(ESI⁺) and NMR spectroscopic data led to determination of the molecular formula as $\text{C}_{19}\text{H}_{18}\text{N}_2\text{O}_4$. In the molecular, the occurrence of a 3-substituted indole nucleus, an *ortho*-substituted benzene ring, two methoxy groups, an isolated methylene, and two ester and amide carbonyl carbons was deduced from analysis of the NMR spectroscopic data (Table 1). The connection of these structural units was further established by the 2D NMR experimental data as illustrated in Fig. 1B. Briefly a linkage between the indole nucleus and one carbonyl carbon via the methylene unit to form a 2-(1*H*-indol-3-yl)acetyl moiety was unambiguously

Table 1
The NMR spectroscopic data (δ) for **CI - 39** in $\text{Me}_2\text{CO}-d_6$ ^a.

no.	δ_{H}	δ_{C}	no.	δ_{H}	δ_{C}
1			1'		116.1
2	7.63 s	124.3	2'		142.3
3		105.1	3'	8.74 d (8.5)	120.6
3a		124.8	4'	7.55 dd (9.0, 8.5)	135.1
4	7.59 d (8.0)	119.8	5'	7.09 dd (9.0, 8.0)	123.1
5	7.06 dd (8.0, 7.5)	120.7	6'	7.91 dd (8.0)	131.5
6	7.22 dd (7.5, 8.0)	123.3	7'		168.7
7	7.46 d (8.0)	109.0	NH	10.92 s	
7a		133.4	OCH ₃	3.72 s	52.6
8	3.87 s	35.7	NOCH ₃	4.19 s	66.4
9		170.7			

^a Chemical shift values (δ) were measured at 500 MHz for ^1H and at 125 MHz for ^{13}C , respectively. Proton coupling constants (J) in Hz are given in parentheses. The assignments were based on DEPT, $^1\text{H}-^1\text{H}$ COSY, HSQC, and HMBC experiments.

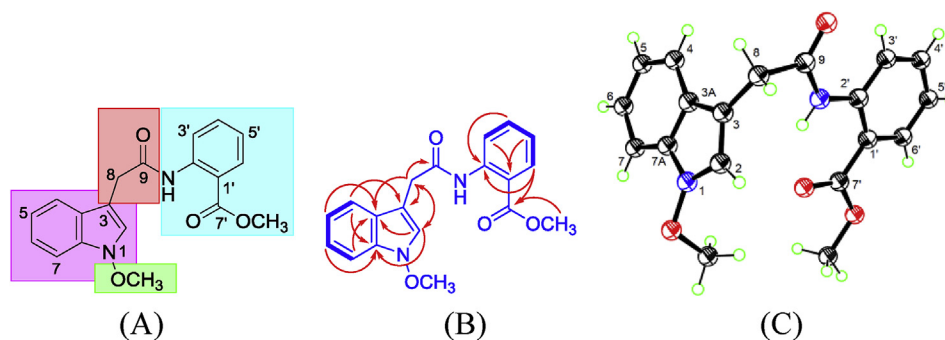


Fig. 1. (A) Structure of the lead compound **CI - 39**; (B) main $^1\text{H}-^1\text{H}$ COSY (thick lines) and HMBC correlations (red arrows, from ^1H to ^{13}C); (C) crystal structure of **CI - 39**. (For interpretation of the references to color in this figure legend, the reader is referred to the Web version of this article.)

established by cross-peaks H-4/H-5/H-6/H-7 in the ^1H - ^1H COSY spectrum as well as the two- and three-bond heteronuclear correlations from H-2 to C-3, C-3a, C-7a, and C-8 and from H₂-8 to C-2, C-3, C-3a, and C-9 in the HMBC spectrum, along with the chemical shifts of these proton and carbon signals (Fig. 1B). Location of a methoxyformyl at the *ortho*-substituted benzene ring to construct a methyl *ortho*-substituted benzoate moiety was deduced from the ^1H - ^1H COSY coupling correlations of H-3'/H-4'/H-5'/H-6' and the long-range HMBC correlations from H-3' to C-1' and C-5' and from H-6' to C-2', C-4, and C-7' as well as from OCH₃ to C-7'. To satisfy the requirement of the molecular composition, the remaining methoxy unit must be located at the *N* atom of the 2-(1*H*-indol-3-yl)acetyl moiety, in turn which must link via an amide bond to the only opened position of the methyl *ortho*-substituted benzoate moiety. The deduction was finally proved by X-ray diffraction analysis of a suitable single crystal crystallized in the acetone solution of **CI-39**, an ORTEP drawn of the crystal structure shown in Fig. 1C. Thus, the structure of **CI-39** was determined as methyl (1-methoxy-1*H*-indol-3-yl)acetamidobenzoate.

According to clinic application of "Ban lan gen" (*I. indigotica* root) in traditional Chinese medicine [17], anti-viral activity of **CI-39** was assayed using cell-based protocols as reported in our previous publications [20–34,56]. This compound showed significant effects on H3N2 (influenza virus A/Hanfang/359/95, EC₅₀ = 2.59 μM), HSV-1 (herpes simplex virus 1, EC₅₀ = 0.95 μM), Coxsackie virus B3 (EC₅₀ = 3.70 μM), and HIV-1 (EC₅₀ = 3.40 μM).

2.1.2. Synthesis of **CI-39** and its inhibitory activity against RT RNA-dependent DNA polymerase

The synthesis of **CI-39** is shown in Scheme 1. Methyl 2-(2-(1*H*-indol-3-yl)acetamido)benzoate (**CI-a**) was obtained through an amidation reaction of indole-3-carboxylic acid with 2-aminobenzoate. Methyl 2-(2-(indolin-3-yl)acetamido)benzoate (**CI-b**) was prepared through reduction using trifluoroacetic acid and triethylsilane [57]. The oxidation of **CI-b** was carried out by sodium tungstate and hydrogen peroxide to produce methyl 2-(2-(1-hydroxy-1*H*-indol-3-yl)acetamido)benzoate (**CI-c**) [58]. Then, the methylation of **CI-c** with trimethylsilyldiazomethane produced **CI-39**.

With the synthesized **CI-39**, inhibitory activities against RT RNA-dependent DNA polymerase [59] and ribonuclease H [60] were detected, along with an activity test against VSVG/HIV-1 replication [56]. The result (Table 3) indicated that **CI-39** was an inhibitor of the RT RNA-dependent DNA polymerase with the IC₅₀ value of 7.20 μM, but inactive to ribonuclease H (IC₅₀ > 30 μM).

2.1.3. Structural modification of **CI-39**

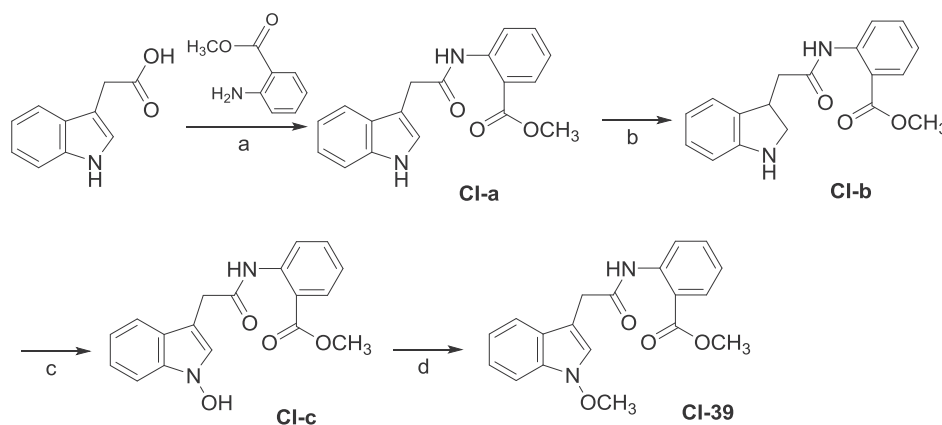
The synthesis of *N*-alkoxy indole derivatives is shown in Scheme 2. The first two steps to obtain the intermediates **2**, **3**, **7** and **8** are as same as the method of preparing **CI-a**, **CI-b**. The oxidation of **3** was carried out by *m*-CPBA to produce an indole *N*-hydroxyl derivative (**4**) [61]. The methylation of **4** with trimethylsilyldiazomethane produced the target product (**5**), and **6** was synthesized from **4** in the presence of potassium carbonate and a halogenated alkane. The intermediates **8** were transformed into the indole *N*-hydroxyl derivative (**9**) through an oxidation reaction using sodium tungstate and hydrogen peroxide. Then, alkylation of **9** under the basic condition provided **10** (Scheme 3).

The synthesis of **14** and **15** is depicted in Scheme 4. The intermediate (**13**) was prepared sequentially by oxidation of **11** and alkylation of the resulting product **12**. A reaction of **13** with oxalyl chloride and 3-chloro-4-aminopyridine yielded **14**, which was further transformed into **15** by reduction with sodium borohydride. The reaction of indole (**16**) and pyridinecarboxaldehyde under the basic condition [62] afforded **17**, which was sequentially reduced and oxidized to yield the intermediates **19** via **18**. Then, propylation of **19** synthesized **20** (Scheme 5).

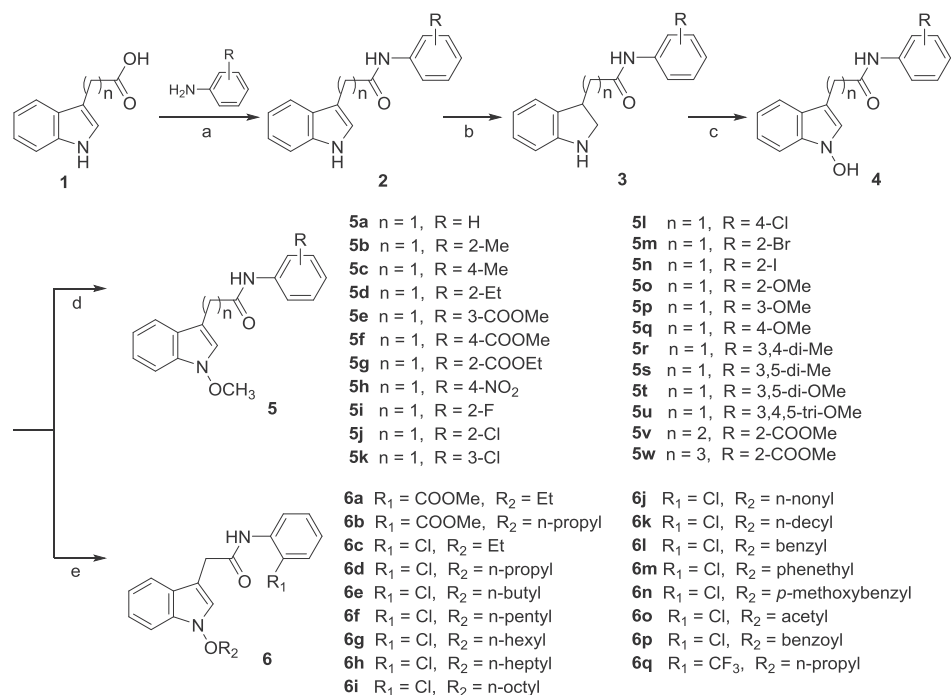
2.1.4. Structure-activity relationships

All the synthesized **CI-39** and 58 derivatives were tested against replication of the wild-type HIV-1 virus and their cytotoxicities on HEK 293T cell as well. As shown in Table 2, replacement of either the *N*-OMe in **CI-39** by *N*-H (**CI-a**) and *N*-OH (**CI-c**) or the indole by an indoline (**CI-b**) resulted in loss of activity. This indicates that the *N*-substituted indole moiety is one of the key pharmacophores. Among the phenylamine ring substituted derivatives (**5**), only those with *ortho*-halogen atoms Cl, Br, and I (**5j**, **5m**, and **5n**) retained activity with the EC₅₀ values of 3.30, 3.20, and 4.40 μM, respectively, whereas all the others (**5a–5i**, **5k**, **5l**, and **5o–5u**) as well as those with the acetyl linker replaced by propionyl and butyryl (**5v** and **5w**) resulted in loss of activity. Accordingly, *ortho*-substitution at the phenylamine moiety by the electron-withdrawing groups (COOMe, Cl, Br, and I) and retention of the acetyl linker are essential to maintain activity.

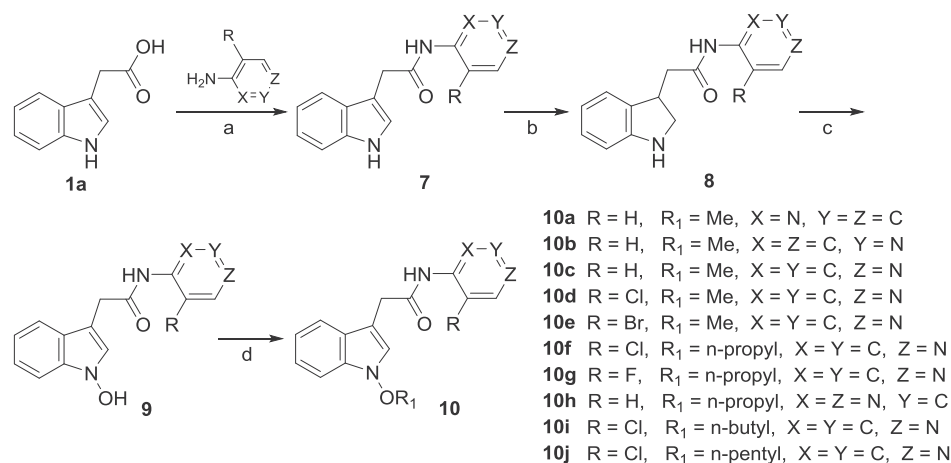
For the *N*-alkoxy-substituted derivatives of **CI-39**, activity was decreased by prolonging the linear alkyl chain (**6a** and **6b**). However, for the halogenated analogues of **5j**, activity was enhanced by extending of the linear alkyl chain from one to five carbon atoms, e.g. methoxy (**5j**: EC₅₀ = 3.30 μM), ethoxy (**6c**: EC₅₀ = 0.86 μM), propoxy (**6d**: EC₅₀ = 0.29 μM), *n*-butoxy (**6e**: EC₅₀ = 0.64 μM), and *n*-pentyloxy (**6f**: EC₅₀ = 0.63 μM). When the number of alkyl linear



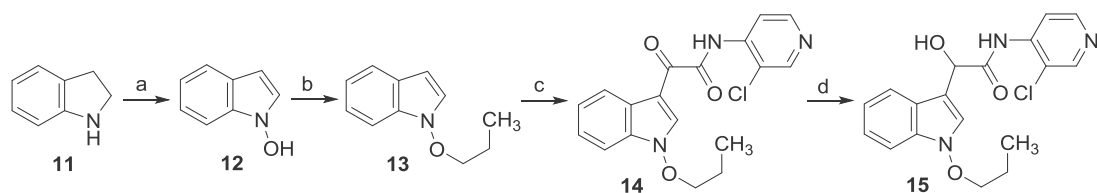
Scheme 1. Synthesis of the natural product **CI-39**. Reagents and conditions: (a) EDCl, DMAP, CH₂Cl₂, r.t.; (b) Et₃SiH, CF₃COOH, reflux; (c) sodium tungstate dihydrate, hydrogen peroxide (30%), MeOH, 0 °C then 15 °C; (d) (trimethylsilyl)diazomethane, CH₂Cl₂, r.t.



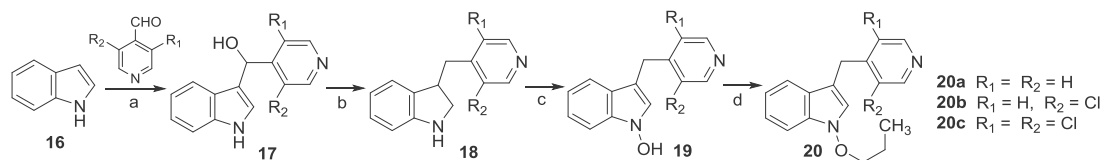
Scheme 2. Synthesis of compounds **5a-5w** and **6a-6q**. Reagents and conditions: (a) EDCI, DMAP, CH_2Cl_2 , r.t.; (b) Et_3SiH , CF_3COOH , reflux; (c) *m*-CPBA, MeOH, 0°C , then r.t.; (d) trimethylsilyldiazomethane, CH_2Cl_2 , r.t.; (e) K_2CO_3 , DMF, r.t..



Scheme 3. Synthesis of compounds **10a-10j**. Reagents and conditions: (a) EDCI, DMAP, CH_2Cl_2 , r.t.; (b) Et_3SiH , CF_3COOH , reflux; (c) sodium tungstate dihydrate, hydrogen peroxide (30%), MeOH, 0°C then 15°C ; (d) (trimethylsilyl)diazomethane, CH_2Cl_2 , r.t. or K_2CO_3 , DMF, r.t..



Scheme 4. Synthesis of compounds **14** and **15**. Reagents and conditions: (a) sodium tungstate dihydrate, hydrogen peroxide (30%), MeOH, 0°C then 15°C ; (b) K_2CO_3 , DMF, r.t.; (c) $(\text{COCl})_2$, Et_2O , 0°C to r.t.; then TEA, 4-amino-3-chloropyridine, CH_2Cl_2 , 0°C to r.t.; (d) sodium borohydride, MeOH, r.t..



Scheme 5. Synthesis of target compounds **20a-20c**. Reagents and conditions: (a) NaOH, MeOH, r.t.; (b) Et₃SiH, CF₃COOH, reflux; (c) sodium tungstate dihydrate, hydrogen peroxide (30%), MeOH, 0 °C then 15 °C; (d) K₂CO₃, DMF, r.t.

carbon atoms exceeded to six, the HIV-1 virus replication inhibitions were gradually decreased (**6g**: EC₅₀ = 1.02 μM; **6h**: EC₅₀ = 1.95 μM; **6i**: EC₅₀ = 4.40 μM), and completely lost when the carbon atom number reached to 9 (**6j**). In addition, introduction of the bulky units at the *N*-atom of the indole moiety also weakened activity, e.g. benzyloxy (**6l**: EC₅₀ = 8.55 μM), phenethyloxy (**6m**: EC₅₀ = 5.50 μM), and *p*-methoxybenzyloxy (**6n**). Complete loss of activity was observed also when electron-withdrawing acetyloxy or benzyloxy substituted at the *N*-atom of the indole moiety (**6o** and **6p**). Interestingly, as compared with **6d** (EC₅₀ = 0.29 μM), the potency was decreased by *ortho*-substitution of the electron-withdrawing group CF₃ on the phenylamine moiety (**6q**: EC₅₀ = 4.28 μM), which differed from **5j**, **5m**, and **5n**. The aforementioned results indicate that the *N*-alkoxy in the **CI - 39** derivatives is required for activity against the HIV-1 virus replication, and the best activity is gained when the number of the linear alkyl carbon atoms is three (**6d**: EC₅₀ = 0.29 μM).

With replacement of the phenylamine moiety by pyridinamines (**10a-10c**), activity was retained only for the derivative of pyridine-4-amine (**10c**: EC₅₀ = 4.95 μM). Simultaneous introduction of Cl or Br at the *ortho*-position of the amino group in the pyridine-4-amine moiety led to a remarkable gain of activity by almost an order of magnitude (**10d**: EC₅₀ = 0.53 μM and **10e**: EC₅₀ = 0.66 μM). Further substitution of *N*-methoxy by *N*-propoxy (**10f**: EC₅₀ = 0.06 μM) or *N*-butoxy (**10i**: EC₅₀ = 0.06 μM) increased activity by one more order of magnitude, while relatively less increase of activity was observed by substitution of *N*-methoxy with *N*-pentyloxy (**10j**: EC₅₀ = 0.13 μM). In addition, as compared with **10f**, activity was reduced by an *ortho*-fluorine substituent on the pyridine-4-amine moiety (**10g**: EC₅₀ = 0.33 μM) or by hydroxylation of the acetyl linker (**15**: EC₅₀ = 2.01 μM). Moreover, comparison of **6d** (EC₅₀ = 0.29 μM) and **10h** (EC₅₀ = 3.30 μM) indicated that replacement of 2-chloroaniline by pyrimidin-4-amine reduced activity by an order of magnitude. Further modification of the acetyl linker through oxidation (**14**) and replacement with a methylene unit (**20**) resulted in the disappearance of activity. Therefore, in the synthesized derivatives the 3-chloropyridin-4-amine moiety is optimal to replace the methyl 2-aminobenzoate moiety in the natural product **CI - 39**. The three potent compounds **6d**, **10f**, and **10i** were selected for following investigations. Notably, we discovered that the intermediate **4o** (ZT55, inactive to HIV-1) was a highly-selective tyrosine kinase inhibitor of JAK2^{V617F} against myeloproliferative neoplasms [63] while other derivatives were inactive at 10 μM. As shown in Table 2, all compounds cytotoxicity was tested, and the cell viabilities were influenced somehow by treating with the compounds at the maximum concentration of 30 μM; nevertheless, the CC₅₀ of all 59 compounds was higher than 10 μM, which was the highest concentration on anti-HIV replication assay.

2.2. Biology

The time-of-drug addition (TOA) assay was conducted to identify the stage at which the active compounds had the inhibitory

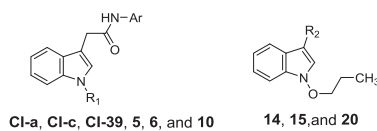
effects on HIV-1. The reverse transcriptase inhibitors zidovudine (AZT) and EFV, and the integrase inhibitor raltegravir (RAL) were used as reference drugs. The assay showed that the activity lost curves of **6d**, **10f**, and **10i** were close to those of AZT and EFV. They had a range of time of 50% failure (FT₅₀) from 8.2 to 9.1 h comparable to AZT at 8.5 h and EFV at 9.4 h, which were far ahead of the integrase inhibitor RAL with a FT₅₀ of 12.2 h (Fig. 2), indicating that compounds **6d**, **10f** and **10i** inhibit HIV-1 replication at the reverse transcription step.

Reverse transcription is a process of generating double-stranded proviral DNA with an HIV-1 RNA genome as the template. This complex process is preceded by RT catalysis with DNA polymerase and Ribonuclease H activities, during which (–)DNA strand is generated by DNA polymerase activity based on the template RNA and the template RNA is hydrolyzed by Ribonuclease H [64,65]. Since the lead compound **CI - 39** was proved as a RT DNA polymerase inhibitor, we also tested the effects of compounds **6d**, **10f** and **10i** on both HIV-1 RT DNA polymerase and Ribonuclease H activities. As shown in Table 3, all three compounds displayed inhibitory activity on RT RNA-dependent DNA polymerase, but not on Ribonuclease H, which indicated that compounds **6d**, **10f**, and **10i** were RT DNA polymerase inhibitors.

HIV-1 RT comprises two subunits p66 and p51. The p66 is the catalytic subunit designated as fingers, palm, thumb, connection, and RNase H domains [66]. All members of approved NNRTIs are RT-DNA polymerase inhibitors by binding to a hydrophobic pocket located between the base of the thumb and the β-sheets of the palm domain, about 10 Å under the catalytic active center. Due to the low fidelity of HIV-1 replication and over two decades of NNRTIs use in clinic, the NNRTI-resistant mutants have developed. Among these, K103N, Y181C or Y188L, carried by RT, are the most prevalent mutants [67]. Lys103 locates on the outer rim of the NNRTI-binding pocket and in the vicinity of the entrance to the pocket; Tyr181 and Tyr188 locates at NNRTI-binding pocket. When Lys103 changes to asparagine, the RT catalytic pocket is preferred in its closed form, resulting in less electrostatic forces within the NNRTIs [68]. Both Tyr181 and Tyr188 exist at the catalytic pocket, which the NNRTIs act on through the π-π interaction of their aromatic rings. As the mutations of Y181C or Y188L occur, the forces between NNRTIs and RT by π-π interaction disappear [69]. For novel NNRTIs, the activity against existing NNRTI-resistant HIV-1 is a pivotal characteristic.

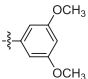
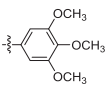
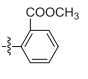
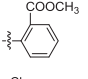
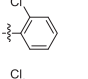
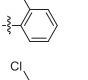
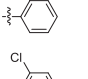
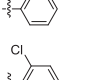
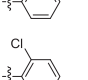
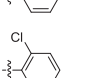
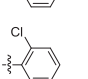
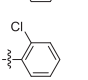
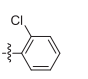
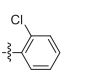
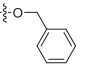
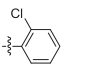
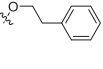
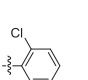
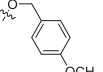
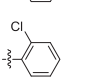
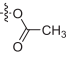
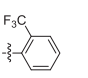
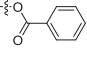
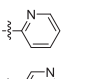
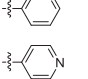


In this study, we evaluated the activities of the natural product **CI - 39** and the potent derivatives **6d**, **10f**, and **10i** against replication of the seven NNRTI-resistant HIV-1 strains. Overall, **10f** and **10i** exhibited better activities and drug resistance folds compared to NVP against six of the seven resistant strains (Table 4). Particularly, **10i** (EC₅₀ = 0.43 μM) was more notably more active against the double mutant L100I/K103N comparing to both NVP (EC₅₀ = 0.76 μM) and EFV (EC₅₀ = 1.08 μM). It is worth noting that the natural product **CI - 39** is the only one fully active on all the viral mutants though it did not exhibit the best activity among the four tested compounds.

Table 2
The effect of the compounds against wild type HIV-1 replication^a.



Compd	Ar	R ₁	R ₂	EC ₅₀ ±SD, μM	CC ₅₀ ±SD, μM	SI
Cl - 39		-OCH ₃	-	3.40 ± 0.45	>30; (51.95 ± 4.29%)	>8.82
Cl-a		-H	-	>10; (91.98 ± 0.02%)	>30; (65.50 ± 5.49%)	-
Cl-b^d	-	-	-	>10; (82.96 ± 1.07%)	>30; (71.46 ± 4.41%)	-
Cl-c		-OH	-	>10; (107.10 ± 7.63%)	24.60 ± 3.79	-
5a		-OCH ₃	-	>10; (113.22 ± 0.48%)	27.98 ± 5.24	-
5b		-OCH ₃	-	>10; (53.31 ± 3.18%)	>30; (62.74 ± 0.54%)	-
5c		-OCH ₃	-	>10; (124.35% ± 9.01%)	>30; (52.47 ± 5.34%)	-
5d		-OCH ₃	-	>10; (64.33 ± 0.23%)	>30; (68.50 ± 3.46%)	-
5e		-OCH ₃	-	>10; (109.33 ± 7.81%)	>30; (50.46 ± 1.22%)	-
5f		-OCH ₃	-	>10; (104.33 ± 3.96%)	>30; (72.64 ± 4.42%)	-
5g		-OCH ₃	-	>10; (60.76 ± 0.94%)	29.08 ± 0.07	-
5h		-OCH ₃	-	>10; (81.41 ± 3.79%)	>30; (54.00 ± 3.54%)	-
5i		-OCH ₃	-	>10; (72.89 ± 1.06%)	28.58 ± 1.78	-
5j		-OCH ₃	-	3.30 ± 0.30	27.78 ± 3.57	8.42
5k		-OCH ₃	-	>10; (113.00 ± 3.13%)	>30; (61.02 ± 5.24%)	-
5l		-OCH ₃	-	>10; (103.55 ± 3.27%)	>30; (51.01 ± 2.25%)	-
5m		-OCH ₃	-	3.20 ± 0.40	>30; (83.48 ± 5.27%)	>9.38
5n		-OCH ₃	-	4.40 ± 0.45	>30; (67.04 ± 0.06%)	>6.82
5o		-OCH ₃	-	>10; (71.46 ± 4.62%)	>30; (59.57 ± 0.05%)	-
5p		-OCH ₃	-	>10; (104.29 ± 0.82%)	>30; (86.68 ± 6.56%)	-
5q		-OCH ₃	-	>10; (128.61 ± 0.08%)	>30; (86.09 ± 7.19%)	-
5r		-OCH ₃	-	>10; (95.02 ± 2.76%)	>30; (51.62 ± 0.34%)	-
5s		-OCH ₃	-	>10; (87.28 ± 5.47%)	>30; (62.62 ± 4.79%)	-

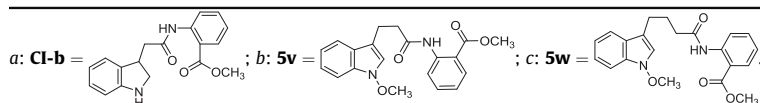
Table 2 (continued)

Compd	Ar	R ₁	R ₂	EC ₅₀ ±SD, μM	CC ₅₀ ±SD, μM	SI
5t		-OCH ₃	-	>10; (98.07 ± 0.36%)	21.63 ± 0.07	-
5u		-OCH ₃	-	>10; (47.94 ± 3.62%)	13.86 ± 1.25	-
5v ^b	-	-	-	>10; (74.25 ± 7.59%)	26.76 ± 1.50	-
5w ^c	-	-	-	>10; (82.07 ± 1.79%)	>30; (61.31 ± 3.32%)	-
6a		-OCH ₂ CH ₃	-	5.70 ± 0.10	>30; (52.76 ± 2.56%)	>5.26
6b		-OCH ₂ CH ₂ CH ₃	-	6.70 ± 0.50	>30; (55.39 ± 2.79%)	>4.48
6c		-OCH ₂ CH ₃	-	0.86 ± 0.04	20.81 ± 2.13	24.20
6d		-OCH ₂ CH ₂ CH ₃	-	0.29 ± 0.01	29.49 ± 1.37	101.69
6e		-O(CH ₂) ₃ CH ₃	-	0.64 ± 0.03	29.14 ± 0.74	45.53
6f		-O(CH ₂) ₄ CH ₃	-	0.63 ± 0.03	18.73 ± 2.18	29.73
6g		-O(CH ₂) ₅ CH ₃	-	1.02 ± 0.08	>30; (56.95 ± 2.10%)	>29.41
6h		-O(CH ₂) ₆ CH ₃	-	1.95 ± 0.05	23.88 ± 1.90	12.25
6i		-O(CH ₂) ₇ CH ₃	-	4.40 ± 0.50	22.93 ± 3.21	5.21
6j		-O(CH ₂) ₈ CH ₃	-	>10; (58.30 ± 1.62%)	28.85 ± 1.16	-
6k		-O(CH ₂) ₉ CH ₃	-	>10; (97.73 ± 1.22%)	>30; (52.80 ± 0.76%)	-
6l			-	8.55 ± 0.95	16.50 ± 1.79	1.93
6m			-	5.50 ± 0.60	>30; (49.31 ± 3.58%)	>5.45
6n			-	>10; (73.20 ± 8.14%)	20.28 ± 236	-
6o			-	>10; (146.89 ± 10.59%)	28.06 ± 0.11	-
6p			-	>10; (113.06 ± 0.17%)	29.43 ± 0.15	-
6q		-OCH ₂ CH ₂ CH ₃	-	4.28 ± 0.41	24.85 ± 3.06	5.81
10a		-OCH ₃	-	>10; (138.11 ± 7.25%)	>30; (63.67 ± 4.32%)	-
10b		-OCH ₃	-	>10; (118.26 ± 7.86%)	>30; (78.70 ± 0.91%)	-
10c		-OCH ₃	-	4.95 ± 0.35	14.27 ± 0.15	2.88

(continued on next page)

Table 2 (continued)

Compd	Ar	R ₁	R ₂	EC ₅₀ ±SD, μM	CC ₅₀ ±SD, μM	SI
10d		-OCH ₃	-	0.53 ± 0.01	19.96 ± 0.86	37.66
10e		-OCH ₃	-	0.66 ± 0.06	18.55 ± 0.58	28.11
10f		-OCH ₂ CH ₂ CH ₃	-	0.06 ± 0.0005	16.41 ± 1.32	273.50
10g		-OCH ₂ CH ₂ CH ₃	-	0.33 ± 0.02	14.13 ± 0.13	42.82
10h		-OCH ₂ CH ₂ CH ₃	-	3.30 ± 0.00	17.92 ± 0.01	5.43
10i		-O(CH ₂) ₃ CH ₃	-	0.06 ± 0.0005	22.06 ± 2.01	367.67
10j		-O(CH ₂) ₄ CH ₃	-	0.13 ± 0.00	21.96 ± 1.99	168.92
14	-	-		>10; (131.6 ± 0.60%)	20.92 ± 5.11	-
15	-	-		2.01 ± 0.06	18.98 ± 2.31	9.44
20a	-	-		>10; (99.48 ± 1.49%)	>30; (69.96 ± 0.41%)	-
20b	-	-		>10; (65.67 ± 2.95%)	>30; (67.37 ± 6.75%)	-
20c	-	-		>10; (93.41 ± 1.56%)	>30; (77.47 ± 3.25%)	-
NVP	-	-	-	0.03 ± 0.003	>30; (93.26 ± 0.68%)	>1000.00
EFV	-	-	-	0.0007 ± 0.0002	23.72 ± 4.45	33885.71



EC₅₀: half maximal effective concentration; CC₅₀: 50% cytotoxic concentration; SI: selectivity index.

^a The percentage in parentheses represents the infectivity or cell viability when treated with the compound at a final concentration of 10 μM or 30 μM.

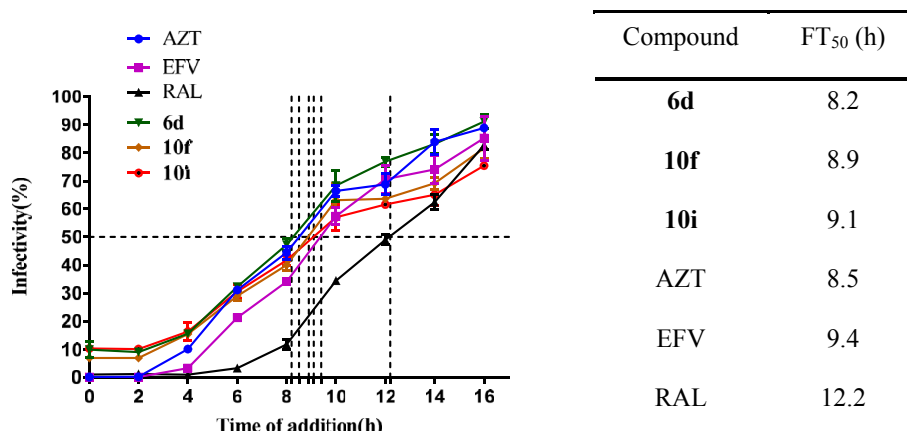


Fig. 2. Time-of-drug addition assay.

Compounds were added at different time points of VSVG/HIV-1 post-infection. The infected cells were lysed 48h post-infection and luciferase activity was measured by FB12 luminometer. The test compounds **6d**, **10f** and **10i**, exhibited the time of 50% failure (FT₅₀) at 8.2, 8.9, and 9.1, respectively; the FT₅₀s of reference compounds AZT, EFV, and RAL were 8.5, 9.4, and 12.2 h, respectively.

Table 3
Effects of **CI - 39**, **6d**, **10f**, and **10i** on HIV-1 RT DNA polymerase and ribonuclease H activities.

Compd	IC ₅₀ ±SD, μM		
	DNA polymerase	Ribonuclease H	VSVG/HIV-1 replication
CI - 39	7.20 ± 0.50	>30	3.37 ± 0.45
6d	0.27 ± 0.03	>100	0.49 ± 0.11
10f	0.11 ± 0.04	>100	0.07 ± 0.02
10i	0.08 ± 0.005	>100	0.04 ± 0.01
HQD	NT	2.81 ± 0.15	NT
NVP	0.98 ± 0.53	NT	0.02 ± 0.003
EFV	0.01 ± 0.003	NT	0.001 ± 0.0001

IC₅₀: half maximal inhibitory concentration; NT: not tested.

2.3. Molecular modeling

In order to better understand the possible binding mode of the active compounds, the potent **10i** and **CI - 39** as well as the positive controls NVP and EFV were docked into the HIV-1 WT RT (PDB code: 1TL1) [69] and the HIV-1 RT mutants RT-Y181C (PDB code: 1JLB) [70], RT-K103N/Y181C (PDB code: 5VQY) [71], and RT-L100I/K103N (PDB code: 2ZE2) [72], respectively. The docking results of **10i** into WT RT (Fig. 3) showed: (i) π -alkyl interactions between the indole ring with Lys103, Leu100, Val179, and Val106; (ii) alkyl interactions between the end of the butoxy chain with Val106, Leu234, Phe227, and Pro225, respectively, in addition to an H-bond between the oxygen-germinal hydrogen on the *N*-alkoxy chain and the Lys101 carbonyl oxygen; (iii) π - π interactions between the pyridine ring with Tyr181, Tyr188, and Trp229, respectively; and (iv) interactions between chlorine with the Tyr181, Pro95, and Leu100 residues. The docking into the Y181C mutated RT (1JLB) (Fig. 4a) indicated that the interaction between chlorine and Tyr181 in WT RT was replaced by a π -alkyl interaction between the

pyridine ring and Cys181, while Tyr188 retained the π - π interaction with the pyridine ring. In addition, the pyridine ring lost its acting force with Leu100, in turn which had a π -sigma interaction with the indole ring. Differently the docking result of **CI - 39** into 1JLB showed that the terminal methyl group of methoxyformyl on the phenylamine moiety shared the π -alkyl interactions with Trp229, Phe227, and Tyr188 and the alkyl interaction with the Leu234 (Fig. S187b in Supporting Information).

Compound **10i** docking into the K103N/Y181C double-mutated RT (5VQY) (Fig. 4b) showed that an H-bond was formed between the Asn103 amide NH₂ group and the *N*-alkoxy oxygen atom, replacing the π -alkyl interaction of the indole ring with Lys103 in WT RT. Meanwhile, the π - π interaction between the pyridine ring and Tyr181 was substituted by a π -sulfur interaction between the indole nucleus and -SH group. Additionally, the pyridine *N* atom hydrogen-bonded to the phenolic hydroxy proton of Tyr188 and the terminal -NH₂ of Lys223, while the pyridine ring maintained the π - π interaction with Tyr188. However, the carbonyl oxygen of methoxyformyl on the phenylamine moiety of **CI - 39** hydrogen-bonded to the terminal -NH₂ of Lys223 and the phenolic hydroxy proton of Tyr188, while Cys181 maintained the same mode of action as **10i** (Fig. S187c in Supporting Information). For the positive control NVP, which is resisted by K103N/Y181C double-mutated RT, the docking simulation (Fig. S185c in Supporting Information) showed no interaction of NVP with Asn103. This suggests that the H-bond between the *N*-alkoxy oxygen atom and the Asn103 amide NH₂ group may play an important role in the effect of **10i**, which is supported by the experimental data (Table 4).

In the case of the L100I/K103N double-mutated RT (Figure 6c), the docking exhibited a position exchange between the indole and pyridine ring moieties in the interacting model, and the hydroxy group from isomerization of the acetamide unit in **10i**

Table 4
Effects of **CI - 39**, **6d**, **10f**, and **10i** on wild type and NNRTI-resistant HIV-1 replication^a.

Virus	EC ₅₀ ±SD, μM						
	CI-39	6d	10f	10i	NVP	EFV	
VSVG/HIV-1 _{wt}	3.37 ± 0.45 (1.0)	0.49 ± 0.11(1.0)	0.07 ± 0.02 (1.0)	0.04 ± 0.01 (1.0)	0.02 ± 0.003 (1.0)	0.001 ± 0.0001 (1.0)	
VSVG/HIV-1 _{RT-K103N}	3.00 ± 0.00 (0.9)	>10 (>20.4)	0.70 ± 0.22 (9.7)	0.72 ± 0.03 (18.7)	1.40 ± 0.19 (81.2)	0.03 ± 0.003 (27.0)	
VSVG/HIV-1 _{RT-Y181C}	2.41 ± 0.02 (0.7)	2.13 ± 0.42 (4.3)	0.18 ± 0.03 (2.5)	0.04 ± 0.01 (1.0)	2.58 ± 0.31 (149.9)	0.002 ± 0.0001 (1.7)	
VSVG/HIV-1 _{RT-K103N,Y181C}	3.08 ± 0.66 (0.9)	>10 (>20.4)	1.85 ± 0.33 (25.7)	0.69 ± 0.08 (17.7)	80.00 ± 9.89 (4657.9)	0.05 ± 0.003 (50.2)	
VSVG/HIV-1 _{RT-L100I,K103N}	2.14 ± 0.29 (0.6)	8.95 ± 1.21 (18.2)	1.18 ± 0.11 (16.3)	0.43 ± 0.04 (11.0)	0.76 ± 0.06 (44.4)	1.08 ± 0.19 (1080.3)	
VSVG/HIV-1 _{RT-Y188L}	3.27 ± 0.44 (1.0)	>10 (>20.4)	1.89 ± 0.22 (26.1)	1.42 ± 0.03 (36.7)	>100 (>5000.0)	0.12 ± 0.03 (124.3)	
VSVG/HIV-1 _{RT-K103N,G190A}	3.19 ± 0.40 (0.9)	>10 (>20.4)	1.38 ± 0.25 (19.2)	0.70 ± 0.11 (18.1)	14.57 ± 0.91 (848.0)	0.18 ± 0.01 (183.0)	
VSVG/HIV-1 _{RT-K103N,V108I}	4.07 ± 0.08 (1.2)	>10 (>20.4)	1.27 ± 0.10 (17.6)	0.56 ± 0.01 (14.5)	2.87 ± 0.35 (167.0)	0.06 ± 0.01 (55.5)	

^a Mean change (fold) in EC₅₀ compared to wild type.

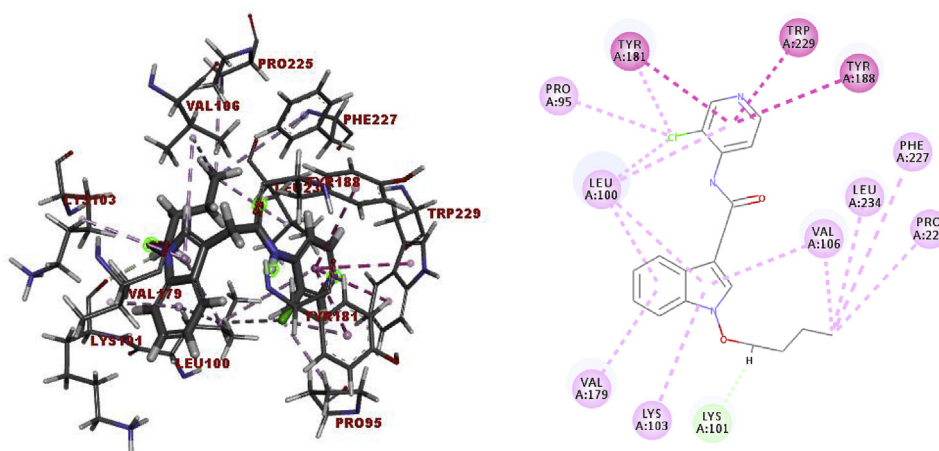


Fig. 3. Binding modes of **10i** into the WT of the HIV-1 RT.

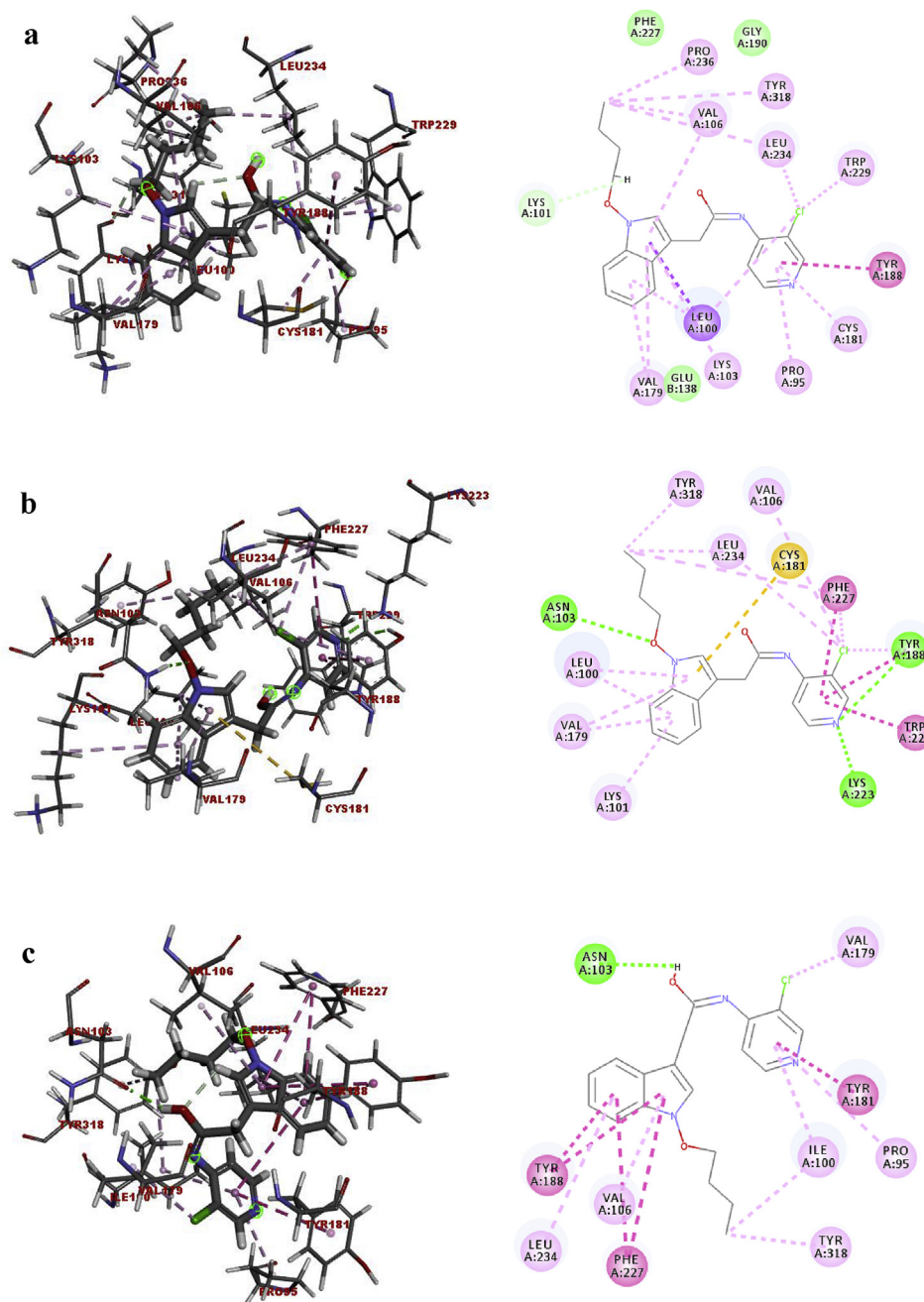


Fig. 4. Binding modes of **10i** into the NNBS of (a) HIV-1 Y181C RT (PDB code: 1JLB); (b) HIV-1 K103N/Y181C RT (PDB code: 5VQY); (c) HIV-1 L100I/K103N RT (PDB code: 2ZE2).

was hydrogen-bonded to the terminal carbamide oxygen of the mutated Asn103. The indole ring began to have a π - π interaction with Tyr188, and the pyridine ring maintained the π - π effect on Tyr181 as well as the acting force with Ile100, in turn which the alkyl- π interaction with the indole nucleus was replaced by an alkyl interaction with the *N*-butoxy chain. Similarly the docking of **CI - 39** displayed the terminal carbamide oxygen of Asn103 hydrogen-bonded to the hydroxy group from isomerization of the acetamide unit (Fig. S187d in Supporting Information). However, the mutated Ile100 exhibited the alkyl interactions with both the methyl group of methoxyformyl and the indole nucleus of **CI - 39**. As the L100I/K103N double-mutated RT resisted EFV, the docking (Fig. S186d in Supporting Information) showed the absence of interaction between the mutated Ile100 and EFV. This suggests that the interactions between **10i/CI - 39**

and the mutated Ile100 are effective on their activities compared to EFV (Table 4).

3. Conclusions

A novel antiviral lead compound **CI - 39** was characterized from an aqueous decoction of the traditional Chinese medicine “ban lan gen” (the *I. indigotica* root), which should have a contribution to the clinical effect of the herbal medicine. Based on the unique structure with potent activity against HIV-1 replication, 57 new derivatives were designed and synthesized, of which 24 were active with EC_{50} values of 0.06–8.55 μ M. Structure-activity relationship of these derivatives was clarified. The biological assays demonstrated that **CI - 39** and its derivatives displayed their activities by inhibiting RT DNA polymerase, but no acting on RNase H. The synthetic

representatives **10f** and **10i** exhibited much better inhibitory effects on the six of seven tested resistant strains compared to NVP. Moreover, the two candidates strongly suppressed NNRTI-resistant HIV-1 carrying the RT-K103N/Y181C mutation. Especially **10i** was superior to both NVP and EFV against the HIV-1_{RT-L1001/K103N}, which suggested that it has the potential for use in developing a new NNRTI. Additionally, the computational docking results also hinted at possible binding mechanisms of the potent **10i**. In summary, this class of derivatives has a good antiviral prospect and deserves further investigation.

4. Experimental

4.1. Chemistry

4.1.1. Isolation and structural determination of **CI - 39**

General experimental procedures, plant material, extraction, and preliminary fractionation of the extract, see Ref. [20]. Fraction C9 (2.8 g) was subjected to CC over Sephadex LH-20 (CHCl₃/MeOH, 1:1) to give C9-1–C9-3, of which C9-2 (1.2 g) was fractionated by RP flash CC (30–70% MeOH in H₂O) to give fractions C9-2-1–C9-2-3. Subfraction C-9-2-1 (500 mg) was separated by CC over silica gel eluting with a gradient of increasing MeOH in CHCl₃ (1–5%) afforded C-9-2-1-1-C-9-2-1-5, of which C-9-2-1-4 (15.4 mg) was isolated by reversed phase HPLC using a semipreparative C18 column and the mobile phase of 33% MeOH in H₂O to yield **CI - 39** (2.1 mg).

4.1.1.1. Methyl (1-methoxy-1H-indol-3-yl)acetamidobenzoate (CI - 39). Yield 0.000042%. M.p. 95–96 °C; UV (MeOH) λ_{\max} (log ϵ) 222(4.81), 252 (4.25), 260 (4.19), 290 (3.99), 300 (3.99) nm; IR (KBr) ν_{\max} 3247, 2948, 2842, 1701, 1677, 1585, 1511, 1452, 1410, 1294, 1264, 1092, 1031, 956, 762, 741 cm⁻¹; ¹H NMR (acetone-*d*₆, 500 MHz) data see Table 1; ¹³C NMR (acetone-*d*₆, 125 MHz) data, see Table 1. ESIMS *m/z* 361 [M + Na]⁺; HR-ESIMS *m/z* 339.1320 [M + H]⁺ (Calcd for C₁₉H₁₉N₂O₄, 339.1339).

4.1.1.2. X-ray crystallography of CI - 39. Molecular formula C₁₉H₁₈N₂O₄, monoclinic, P2₁/c, *a* = 7.449 (3) Å, *b* = 23.336 (12) Å, *c* = 10.026 (4) Å, $\alpha = \gamma = 90^\circ$, $\beta = 93.84(8)^\circ$, *V* = 1738.9 (13) Å³, *Z* = 4, *D*_{calcd} = 1.292 g/cm³, 3391 reflections independent, 2069 reflections observed ($|F|^2 \geq 2\sigma|F|^2$), *R*₁ = 0.0521, *wR*₂ = 0.1246, *S* = 1.004.

The data were collected on a Rigaku MicroMax 002+ diffractometer with CuK α radiation by using the ω and κ scan technique to a maximum 2θ value of 144.60°. The crystal structure was solved by direct methods by using SHELXS-97, and all non-hydrogen atoms were refined anisotropically using the least-squares method. All hydrogen atoms were positioned by geometric calculations. Crystallographic data have been deposited with the Cambridge Crystallographic Data Center (CCDC 866444). Copies of these data can be obtained free of charge via www.ccdc.cam.ac.uk/conts/retrieving.html (or from the Cambridge Crystallographic Data Centre, 12 Union Road, Cambridge CB21EZ, UK; fax: (+44) 1223-336-033; or deposit@ccdc.cam.ac.uk).

4.1.2. Synthesis

All the synthetic starting materials and reagents were purchased from commercial suppliers and used directly without further purification. Column chromatography was performed using silica gel (200–300 mesh) purchased from Qingdao Haiyang Chemical Co., Ltd. Thin-layer chromatography was performed on precoated silica gel F-254 plates and was visualized under UV light. ¹H NMR and ¹³C NMR spectra were recorded on Varian Mercury 300 MHz, 400 MHz or 500 MHz with TMS or solvent peaks as references. Chemical shifts (δ) are reported in parts per million (ppm) and coupling constants (*J*) are reported in hertz (Hz). The splitting

patterns are indicated as: s = singlet, d = doublet, t = triplet, q = quartet, dd = doublet of doublet, m = multiplet. HR-ESIMS data were obtained on an Agilent 6520 Accurate-Mass Q-TOF LCMS spectrometers (Agilent Technologies, Ltd., Santa Clara, CA, USA). Analysis of sample purity was performed on an Agilent HPLC system consisting of 1100 controller, 1100 pump, and 1100 dual λ absorbance detector with an CAPCELL PAK AQ-C18 column (5 μ m, 250 \times 4.6 mm). HPLC conditions: solvent A: H₂O; solvent B: CH₃OH; flow rate 1.0 mL/min; compounds were eluted with a gradient of 30% CH₃OH in H₂O with to 100% CH₃OH for 20 min. All tested compounds have a purity $\geq 95.0\%$.

4.1.2.1. Synthesis of CI - 39. To a solution of indole-3-acetic acid (1.05 g, 1 equiv.) in dry CH₂Cl₂ (100 mL) was added EDCI (1.27 g, 1.1 equiv.). The reaction mixture was stirred at room temperature for 1 h, then methyl 2-aminobenzoate (1.0 g, 1.1 equiv.) and DMAP (0.07 g, 0.1 equiv.) were added. The mixture was stirred at room temperature for 3 h; 2 M hydrochloric acid (100 mL) was added and stirred strongly for 10 min. The organic phase was separated and the water phase was extracted with CH₂Cl₂ (50 mL) twice. The combined organic phase was washed with brine and dried with Na₂SO₄. Filtration and removal of the solvent at 40 °C under reduced pressure yielded methyl 2-(2-(1H-indol-3-yl)acetamido)benzoate (**CI-a**, 1.03 g).

To a solution of **CI-a** (1.03 g, 1 equiv.) in CF₃COOH (30 mL) was added Et₃SiH (1.2 g, 3 equiv.), stirred at 60 °C for 1 h, followed by recovery of the solvent under reduced pressure to yield a residue. The residue was dissolved in ethyl acetate and washed by saturated Na₂CO₃ and brine in order, subsequent removal of the solvent under reduced pressure afforded methyl 2-(2-(indolin-3-yl)acetamido)benzoate (**CI-b**, 0.98 g). To a solution of **CI-b** (0.98 g, 1 equiv.) in MeOH (50 mL) was added sodium tungstate dehydrate (0.3 g, 0.3 equiv.) at 0 °C, followed by dropwise addition of hydrogen peroxide (30%, 3.5 mL, 10 equiv.) then stirred at 10–15 °C for 1 h. The reaction mixture was partitioned between CH₂Cl₂ and water, and the organic phase was washed with brine and evaporated, the resulting residue was purified by column chromatography (silica gel, petroleum ether/ethyl acetate 2:1) to furnish methyl 2-(2-(1-hydroxy-1H-indol-3-yl)acetamido)benzoate (**CI-c**, 0.69 g). Selectively the CH₂Cl₂ solution of **CI-c** (0.69 g) was added a solution of trimethylsilyldiazomethane in n-hexane (6 M, 3.5 mL, 10 equiv.), stirred at room temperature overnight, followed by recovery of the organic solvent to give a residue. The residue was purified by silica gel column chromatography (petroleum ether/ethyl acetate 2:1) to yield **CI - 39** (0.49 g, four steps yield 24.2%).

4.1.2.1.1. Methyl 2-(2-(1H-indol-3-yl)acetamido)benzoate (CI-a) [73]. Yield 55.5%. ¹H NMR (500 MHz, DMSO-*d*₆): δ 11.07 (s, 1H, CONH), 10.59 (s, 1H, NH), 8.41 (d, *J* = 8.5 Hz, 1H, ArH), 7.84 (dd, *J* = 2.0, 8.0 Hz, 1H, ArH), 7.58 (t, *J* = 7.5 Hz, 1H, ArH), 7.51 (d, *J* = 7.5 Hz, 1H, ArH), 7.38 (m, 2H, ArH), 7.10 (m, 2H, ArH), 6.97 (t, *J* = 7.5 Hz, 1H, ArH), 3.83 (s, 2H, CH₂), 3.64 (s, 3H, CH₃). ESIMS *m/z* 331 [M + Na]⁺, 344 [M + Cl]⁻.

4.1.2.1.2. Methyl 2-(2-(indolin-3-yl)acetamido)benzoate (CI-b). Yield 95.0%. ¹H NMR (500 MHz, acetone-*d*₆): δ 11.00 (s, 1H, CONH), 8.74 (d, *J* = 8.5 Hz, 1H, ArH), 8.03 (dd, *J* = 2.0, 8.5 Hz, 1H, ArH), 7.60 (t, *J* = 8.0 Hz, 1H, ArH), 7.13 (m, 2H, ArH), 6.94 (t, *J* = 7.5 Hz, 1H, ArH), 6.57 (m, 2H, ArH), 4.89 (s, 1H, NH), 3.90 (s, 3H, CH₃), 3.75 (m, 2H, CH₂), 3.30 (m, 1H, CH), 2.87 (m, 1H, CH₂), 2.67 (m, 1H, CH₂); ¹³C NMR (125 MHz, acetone-*d*₆): δ 170.9, 169.1, 153.1, 142.3, 135.2, 132.1, 131.6, 128.4, 124.5, 123.2, 120.9, 118.3, 116.0, 109.8, 53.9, 52.8, 43.5, 39.5; HR-ESIMS *m/z* 311.1398 [M + H]⁺ (Calcd for C₁₈H₁₉N₂O₃, 311.1390).

4.1.2.1.3. Methyl 2-(2-(1-hydroxy-1H-indol-3-yl)acetamido)benzoate (CI-c). Yield 67.5%. ¹H NMR (500 MHz, acetone-*d*₆): δ 10.87 (1H, s, NH), 10.21 (1H, s, OH), 8.71 (1H, d, *J* = 8.5 Hz, ArH), 7.93 (1H,

dd, $J = 1.5, 8.0$ Hz, ArH), 7.56 (2H, m, ArH), 7.49 (1H, s, ArH), 7.42 (1H, d, $J = 8.0$ Hz, ArH), 7.17 (1H, t, $J = 7.5$ Hz, ArH), 7.09 (1H, t, $J = 7.5$ Hz, ArH), 7.02 (1H, t, $J = 7.5$ Hz, ArH), 3.86 (2H, s, CH₂), 3.74 (3H, s, COOCH₃); ¹³C NMR (150 MHz, acetone-*d*₆): δ 170.8, 168.2, 142.4, 135.0 (2C), 131.5, 125.8, 124.7, 123.1, 122.8, 120.7, 120.0, 119.6, 116.4, 109.2, 104.2, 52.6, 35.8; HR-ESIMS m/z 325.119 [M + H]⁺ (Calcd for C₁₈H₁₇N₂O₄, 325.1183).

4.1.2.2. General procedure for the synthesis of 5, 6 and 10. The first two steps of general procedure for the synthesis of intermediates **2**, **3**, **7** and **8** are same as that of preparing **Cl-a**, **Cl-b**. To a solution of **3** (1 equiv.) in MeOH was added *m*-CPBA (2 equiv.), stirred at room temperature for 2 h, then concentrated under reduced pressure to yield a residue, which was dissolved in CH₂Cl₂ and washed successively by saturated Na₂CO₃ and brine. The CH₂Cl₂ solution was evaporated and the resulting residue was purified by column chromatography (silica gel, petroleum ether/ethyl acetate 2:1) to furnish **4**. Similarly, **9** was obtained as same as the procedure of prepare **Cl-c**. Selectively the CH₂Cl₂ solution of **4** or **9** was added to a solution of trimethylsilyldiazomethane in *n*-hexane (6 M, 10 equiv) or the alkyl halide (1.5 equiv.), stirred at room temperature overnight or for 2 h in DMF with K₂CO₃ (2 equiv.), followed by partition between CH₂Cl₂ and water, then dry with Na₂SO₄ and recovery of the organic solvent or to give a residue. The residue was purified by silica gel column chromatography (petroleum ether/ethyl acetate 2:1) to yield **5**, **6**, and **10**.

4.1.2.2.1. 2-(1-Methoxy-1H-indol-3-yl)-N-phenylacetamide (5a). Four steps yield 29.6%. ¹H NMR (400 MHz, acetone-*d*₆): δ 9.16 (s, 1H, CONH), 7.64 (m, 3H, ArH), 7.46 (s, 1H, ArH), 7.42 (d, $J = 8.4$ Hz, 1H, ArH), 7.23 (m, 3H, ArH), 7.04 (m, 2H, ArH), 4.05 (s, 3H, OCH₃), 3.79 (s, 2H, CH₂); ¹³C NMR (100 MHz, acetone-*d*₆): δ 169.9, 140.4, 133.4, 129.4 (2C), 124.9, 124.1, 123.4, 123.2, 120.4, 120.2 (2C), 120.1, 109.0, 106.6, 66.1, 34.6; HR-ESIMS m/z 281.1287 [M + H]⁺ (Calcd for C₁₇H₁₇N₂O₂, 281.1285).

4.1.2.2.2. 2-(1-Methoxy-1H-indol-3-yl)-N-(*o*-tolyl)acetamide (5b). Four steps yield 20.0%. ¹H NMR (400 MHz, acetone-*d*₆): δ 8.33 (s, 1H, CONH), 7.72 (d, $J = 8.0$ Hz, 1H, ArH), 7.68 (d, $J = 8.0$ Hz, 1H, ArH), 7.54 (s, 1H, ArH), 7.45 (d, $J = 8.4$ Hz, 1H, ArH), 7.24 (t, $J = 7.6$ Hz, 1H, ArH), 7.10 (m, 3H, ArH), 6.99 (t, $J = 7.6$ Hz, 1H, ArH), 4.10 (s, 3H, OCH₃), 3.84 (s, 2H, CH₂), 2.01 (s, 3H, CH₃); ¹³C NMR (100 MHz, acetone-*d*₆): δ 169.7, 137.6, 133.4, 131.0, 130.7, 126.9, 125.4, 124.8, 124.1, 123.6, 123.3, 120.6, 120.1, 109.0, 106.6, 66.2, 34.3, 17.7; HR-ESIMS m/z 295.1447 [M + H]⁺ (Calcd for C₁₈H₁₉N₂O₂, 295.1441).

4.1.2.2.3. 2-(1-Methoxy-1H-indol-3-yl)-N-(*p*-tolyl)acetamide (5c). Four steps yield 27.8%. ¹H NMR (400 MHz, acetone-*d*₆): δ 9.11 (s, 1H, CONH), 7.66 (d, $J = 8.0$ Hz, 1H, ArH), 7.51 (d, $J = 8.4$ Hz, 2H, ArH), 7.44 (s, 1H, ArH), 7.41 (d, $J = 8.4$ Hz, 1H, ArH), 7.21 (t, $J = 8.0$ Hz, 1H, ArH), 7.06 (t, 3H, ArH), 4.06 (s, 3H, OCH₃), 3.77 (s, 2H, CH₂), 2.24 (s, 3H, CH₃); ¹³C NMR (100 MHz, acetone-*d*₆): δ 169.7, 137.8, 133.3, 129.8 (2C), 124.9, 123.4, 123.1, 120.4, 120.2, 108.9, 106.7, 66.1, 34.6, 20.7; HR-ESIMS m/z 295.145 [M + H]⁺ (Calcd for C₁₈H₁₉N₂O₂, 295.1441).

4.1.2.2.4. N-(2-Ethylphenyl)-2-(1-methoxy-1H-indol-3-yl)acetamide (5d). Four steps yield 27.8%. ¹H NMR (400 MHz, acetone-*d*₆): δ 8.20 (s, 1H, CONH), 7.76 (d, $J = 8.0$ Hz, 1H, ArH), 7.68 (d, $J = 8.0$ Hz, 1H, ArH), 7.57 (s, 1H, ArH), 7.46 (d, $J = 7.6$ Hz, 1H, ArH), 7.25 (t, $J = 7.6$ Hz, 1H, ArH), 7.11 (m, 3H, ArH), 7.03 (t, $J = 6.8$ Hz, 1H, ArH), 4.12 (s, 3H, OCH₃), 3.84 (s, 2H, CH₂), 2.33 (q, $J = 7.6, 14.8$ Hz, 2H, CH₂), 0.85 (t, 3H, $J = 7.6$ Hz, CH₃); ¹³C NMR (100 MHz, acetone-*d*₆): δ 169.8, 136.8, 136.4, 133.4, 129.4, 126.9, 125.7, 124.7, 124.4, 123.7, 123.5, 120.7, 120.1, 109.1, 106.5, 66.3, 34.4, 24.7, 14.3; HR-ESIMS m/z 309.1601 [M + H]⁺ (Calcd for C₁₉H₂₁N₂O₂, 309.1598).

4.1.2.2.5. Methyl 3-[2-(1-methoxy-1H-indol-3-yl)acetamido]benzoate (5e). Four steps yield 21.4%. ¹H NMR (400 MHz, acetone-*d*₆): δ 9.37 (s, 1H, CONH), 8.29 (s, 1H, ArH), 7.89 (d, $J = 8.0$ Hz, 1H, ArH),

7.67 (d, $J = 7.6$ Hz, 2H, ArH), 7.48 (s, 1H, ArH), 7.40 (m, 2H, ArH), 7.21 (t, $J = 7.6$ Hz, 1H, ArH), 7.06 (t, $J = 7.6$ Hz, 1H, ArH), 4.09 (s, 3H, OCH₃), 3.84 (s, 3H, COOCH₃), 3.83 (s, 2H, CH₂); ¹³C NMR (100 MHz, acetone-*d*₆): δ 170.2, 167.0, 140.6, 133.4, 131.6, 129.7, 124.9, 124.86, 124.4, 123.5, 123.2, 120.9, 120.5, 120.1, 109.0, 106.3, 66.2, 52.3, 34.6; HR-ESIMS m/z 339.1347 [M + H]⁺ (Calcd for C₁₉H₁₉N₂O₄, 339.1339).

4.1.2.2.6. Methyl 4-[2-(1-methoxy-1H-indol-3-yl)acetamido]benzoate (5f). Four steps yield 24.7%. ¹H NMR (400 MHz, acetone-*d*₆): δ 9.49 (s, 1H, CONH), 7.92 (d, 2H, $J = 8.4$ Hz, ArH), 7.76 (d, $J = 8.4$ Hz, 2H, ArH), 7.65 (d, $J = 8.0$ Hz, 1H, ArH), 7.46 (s, 1H, ArH), 7.41 (d, $J = 8.0$ Hz, 1H, ArH), 7.21 (t, $J = 7.6$ Hz, 1H, ArH), 7.07 (t, $J = 7.6$ Hz, 1H, ArH), 4.10 (s, 3H, OCH₃), 3.84 (s, 2H, CH₂), 3.83 (s, 3H, COOCH₃); ¹³C NMR (100 MHz, acetone-*d*₆): δ 170.5, 166.7, 144.5, 133.3, 131.1 (2C), 125.6, 124.8, 123.5, 123.2, 120.5, 120.1, 119.3 (2C), 109.0, 106.1, 66.1, 52.0, 34.7; HR-ESIMS m/z 339.1344 [M + H]⁺ (Calcd for C₁₉H₁₉N₂O₄, 339.1339).

4.1.2.2.7. Ethyl 2-[2-(1-methoxy-1H-indol-3-yl)acetamido]benzoate (5g). Four steps yield 20.0%. ¹H NMR (400 MHz, acetone-*d*₆): δ 11.00 (s, 1H, CONH), 8.76 (d, $J = 8.4$ Hz, 1H, ArH), 7.92 (d, $J = 8.0$ Hz, 1H, ArH), 7.60 (s, 1H, ArH), 7.59 (d, $J = 9.2$ Hz, 1H, ArH), 7.53 (t, $J = 8.0$ Hz, 1H, ArH), 7.46 (d, $J = 8.0$ Hz, 1H, ArH), 7.21 (t, $J = 7.6$ Hz, 1H, ArH), 7.06 (m, 2H, ArH), 4.180 (m, 5H, CH₂, OCH₃), 3.87 (s, 2H, CH₂), 1.25 (t, $J = 6.8$ Hz, 3H, CH₃); ¹³C NMR (100 MHz, acetone-*d*₆): δ 170.7, 168.2, 142.4, 134.9, 133.3, 131.5, 124.8, 124.2, 123.3, 123.0, 120.6, 120.5, 119.8, 116.2, 109.0, 105.1, 66.4, 61.9, 35.7, 14.3; HR-ESIMS m/z 353.1504 [M + H]⁺ (Calcd for C₂₀H₂₁N₂O₄, 353.1496).

4.1.2.2.8. 2-(1-Methoxy-1H-indol-3-yl)-N-(4-nitrophenyl)acetamide (5h). Four steps yield 25.9%. ¹H NMR (400 MHz, acetone-*d*₆): δ 9.76 (s, 1H, CONH), 8.17 (d, $J = 9.2$ Hz, 2H, ArH), 7.88 (d, $J = 8.8$ Hz, 2H, ArH), 7.64 (d, $J = 7.6$ Hz, 1H, ArH), 7.49 (s, 1H, ArH), 7.42 (d, $J = 7.6$ Hz, 1H, ArH), 7.21 (t, $J = 7.6$ Hz, 1H, ArH), 7.07 (t, $J = 7.2$ Hz, 1H, ArH), 4.09 (s, 3H, OCH₃), 3.88 (s, 2H, CH₂); ¹³C NMR (100 MHz, acetone-*d*₆): δ 170.8, 146.3, 143.8, 133.3, 125.5 (2C), 124.8, 123.6, 123.3, 120.5, 120.1, 119.7 (2C), 109.0, 105.8, 66.2, 34.7; HR-ESIMS m/z 326.1144 [M + H]⁺ (Calcd for C₁₇H₁₆N₂O₄, 326.1135).

4.1.2.2.9. N-(2-Fluorophenyl)-2-(1-methoxy-1H-indol-3-yl)acetamide (5i). Four steps yield 18.5%. ¹H NMR (400 MHz, acetone-*d*₆): δ 8.83 (s, 1H, CONH), 8.22 (t, $J = 8.0$ Hz, 1H, ArH), 7.68 (d, $J = 8.0$ Hz, 1H, ArH), 7.52 (s, 1H, ArH), 7.44 (d, $J = 8.0$ Hz, 1H, ArH), 7.22 (t, $J = 7.6$ Hz, 1H, ArH), 7.09 (m, 4H, ArH), 4.09 (s, 3H, OCH₃), 3.91 (s, 2H, CH₂); ¹³C NMR (100 MHz, acetone-*d*₆): δ 170.1, 133.4, 125.2, 125.14, 125.09, 125.06, 124.8, 123.5, 123.4, 123.3, 120.5, 120.1, 115.8, 115.6, 109.0, 106.3, 66.2, 34.3; HR-ESIMS m/z 299.1193 [M + H]⁺ (Calcd for C₁₇H₁₆N₂O₂F, 299.1190).

4.1.2.2.10. N-(2-Chlorophenyl)-2-(1-methoxy-1H-indol-3-yl)acetamide (5j). Four steps yield 22.0%. ¹H NMR (400 MHz, acetone-*d*₆): δ 8.46 (s, 1H, CONH), 8.29 (d, $J = 8.0$ Hz, 1H, ArH), 7.67 (d, $J = 8.0$ Hz, 1H, ArH), 7.61 (s, 1H, ArH), 7.47 (d, $J = 8.0$ Hz, 1H, ArH), 7.33 (d, $J = 8.0$ Hz, 1H, ArH), 7.26 (m, 2H, ArH), 7.10 (t, $J = 7.6$ Hz, 1H, ArH), 7.05 (t, $J = 8.0$ Hz, 1H, ArH), 4.12 (s, 3H, OCH₃), 3.925 (s, 2H, CH₂); ¹³C NMR (100 MHz, acetone-*d*₆): δ 169.9, 136.1, 133.4, 129.9, 128.3, 125.5, 124.7, 123.9, 123.5, 122.9 (2C), 120.8, 120.0, 109.1, 105.8, 66.3, 34.5; HR-ESIMS m/z 315.0905 [M + H]⁺ (Calcd for C₁₇H₁₆N₂O₂Cl, 315.0895).

4.1.2.2.11. N-(3-Chlorophenyl)-2-(1-methoxy-1H-indol-3-yl)acetamide (5k). Four steps yield 23.1%. ¹H NMR (400 MHz, acetone-*d*₆): δ 9.33 (s, 1H, CONH), 7.89 (s, 1H, ArH), 7.64 (d, $J = 8.0$ Hz, 1H, ArH), 7.44 (m, 3H, ArH), 7.26 (t, $J = 8.0$ Hz, 1H, ArH), 7.21 (t, $J = 8.0$ Hz, 1H, ArH), 7.06 (m, 2H, ArH), 4.09 (s, 3H, OCH₃), 3.80 (s, 2H, CH₂); ¹³C NMR (100 MHz, acetone-*d*₆): δ 170.3, 141.7, 134.6, 133.3, 130.9, 124.8, 123.9, 123.5, 123.2, 120.5, 120.1, 119.9, 118.3, 109.0, 106.2, 66.2, 34.6; HR-ESIMS m/z 315.0897 [M + H]⁺ (Calcd for C₁₇H₁₆N₂O₂Cl, 315.0895).

4.1.2.2.12. N-(4-Chlorophenyl)-2-(1-methoxy-1H-indol-3-yl)acetamide (5l). Four steps yield 20.4%. ¹H NMR (400 MHz, acetone-*d*₆):

δ 9.30 (s, 1H, CONH), 7.65 (m, 3H, ArH), 7.46 (s, 1H, ArH), 7.41 (d, $J = 8.4$ Hz, 1H, ArH), 7.27 (d, $J = 8.4$ Hz, 2H, ArH), 7.21 (t, $J = 7.6$ Hz, 1H, ArH), 7.06 (t, $J = 7.6$ Hz, 1H, ArH), 4.08 (s, 3H, OCH₃), 3.79 (s, 2H, CH₂); ¹³C NMR (100 MHz, acetone-*d*₆): δ 170.1, 139.2, 133.3, 129.3 (2C), 128.4, 124.8, 123.5, 123.2, 121.6 (2C), 120.5, 120.1, 109.0, 106.3, 66.2, 34.6; HR-ESIMS m/z 315.0905 [M + H]⁺ (Calcd for C₁₇H₁₆N₂O₂Cl, 315.0895).

4.1.2.2.13. *N*-(2-Bromophenyl)-2-(1-methoxy-1*H*-indol-3-yl)acetamide (5m). Four steps yield 11.1%. ¹H NMR (400 MHz, acetone-*d*₆): δ 8.32 (s, 1H, CONH), 8.27 (d, $J = 8.0$ Hz, 1H, ArH), 7.66 (d, $J = 8.0$ Hz, 1H, ArH), 7.64 (s, 1H, ArH), 7.49 (d, $J = 7.6$ Hz, 1H, ArH), 7.47 (d, $J = 8.0$ Hz, 1H, ArH), 7.32 (t, $J = 8.0$ Hz, 1H, ArH), 7.25 (t, $J = 7.6$ Hz, 1H, ArH), 7.10 (t, $J = 7.6$ Hz, 1H, ArH), 6.99 (t, $J = 8.0$ Hz, 1H, ArH), 4.13 (s, 3H, OCH₃), 3.91 (s, 2H, CH₂); ¹³C NMR (100 MHz, acetone-*d*₆): δ 169.9, 137.2, 133.4, 133.2, 129.0, 126.0, 124.7, 124.0, 123.6, 122.9, 120.9, 120.0, 114.2, 109.1, 105.6, 66.4, 34.6; HR-ESIMS m/z 359.0403 [M + H]⁺ (Calcd for C₁₇H₁₆N₂O₂Br, 359.0390).

4.1.2.2.14. *N*-(2-Iodophenyl)-2-(1-methoxy-1*H*-indol-3-yl)acetamide (5n). Four steps yield 10.3%. ¹H NMR (400 MHz, acetone-*d*₆): δ 8.17 (d, $J = 8.4$ Hz, 1H, ArH), 8.13 (s, 1H, CONH), 7.72 (d, $J = 7.6$ Hz, 1H, ArH), 7.65 (m, 2H, ArH), 7.47 (d, $J = 8.4$ Hz, 1H, ArH), 7.33 (t, $J = 8.0$ Hz, 1H, ArH), 7.25 (t, $J = 8.0$ Hz, 1H, ArH), 7.10 (t, $J = 7.6$ Hz, 1H, ArH), 6.83 (t, $J = 7.6$ Hz, 1H, ArH), 4.14 (s, 3H, OCH₃), 3.89 (s, 2H, CH₂); ¹³C NMR (100 MHz, acetone-*d*₆): δ 169.9, 139.8 (2C), 133.5, 129.7, 126.7, 124.7, 124.2, 123.6, 122.7 (2C), 120.9, 120.1, 109.2, 105.4, 66.5, 34.6; HR-ESIMS m/z 407.0269 [M + H]⁺ (Calcd for C₁₇H₁₆I₂O₂, 407.0251).

4.1.2.2.15. 2-(1-Methoxy-1*H*-indol-3-yl)-*N*-(2-methoxyphenyl)acetamide (5o). Four steps yield 35.2%. ¹H NMR (400 MHz, acetone-*d*₆): δ 8.43 (s, 1H, CONH), 8.33 (d, $J = 7.6$ Hz, 1H, ArH), 7.67 (d, $J = 7.6$ Hz, 1H, ArH), 7.56 (s, 1H, ArH), 7.47 (d, $J = 8.0$ Hz, 1H, ArH), 7.24 (t, $J = 7.6$ Hz, 1H, ArH), 7.10 (t, $J = 7.6$ Hz, 1H, ArH), 6.96 (t, $J = 8.0$ Hz, 1H, ArH), 6.87 (m, 2H, ArH), 4.13 (s, 3H, OCH₃), 3.86 (s, 2H, CH₂), 3.64 (s, 3H, OCH₃); ¹³C NMR (100 MHz, acetone-*d*₆): δ 169.5, 149.1, 133.4, 129.1, 124.7, 124.2, 123.7, 123.4, 121.3, 120.7, 120.13, 120.09, 111.2, 109.1, 106.4, 66.3, 56.0, 34.8; HR-ESIMS m/z 311.1397 [M + H]⁺ (Calcd for C₁₈H₁₉N₂O₃, 311.1390).

4.1.2.2.16. 2-(1-Methoxy-1*H*-indol-3-yl)-*N*-(3-methoxyphenyl)acetamide (5p). Four steps yield 34.6%. ¹H NMR (400 MHz, acetone-*d*₆): δ 9.30 (s, 1H, CONH), 7.66 (d, $J = 8.0$ Hz, 1H, ArH), 7.46 (s, 1H, ArH), 7.41 (d, $J = 6.8$ Hz, 2H, ArH), 7.20 (t, $J = 7.6$ Hz, 1H, ArH), 7.13 (m, 2H, ArH), 7.06 (t, $J = 7.6$ Hz, 1H, ArH), 6.59 (d, $J = 6.8$ Hz, 1H, ArH), 4.08 (s, 3H, OCH₃), 3.78 (s, 2H, CH₂), 3.72 (s, 3H, OCH₃); ¹³C NMR (100 MHz, acetone-*d*₆): δ 169.9, 160.9, 141.6, 133.3, 130.1, 124.9, 123.4, 123.1, 120.4, 120.2, 112.3, 109.5, 108.9, 106.6, 105.9, 66.1, 55.4, 34.6; HR-ESIMS m/z 311.1399 [M + H]⁺ (Calcd for C₁₈H₁₉N₂O₃, 311.1390).

4.1.2.2.17. 2-(1-Methoxy-1*H*-indol-3-yl)-*N*-(4-methoxyphenyl)acetamide (5q). Four steps yield 32.9%. ¹H NMR (400 MHz, acetone-*d*₆): δ 9.02 (s, 1H, CONH), 7.66 (d, $J = 8.0$ Hz, 1H, ArH), 7.52 (d, $J = 8.8$ Hz, 2H, ArH), 7.45 (s, 1H, ArH), 7.41 (d, $J = 8.0$ Hz, 1H, ArH), 7.20 (t, $J = 7.6$ Hz, 1H, ArH), 7.06 (t, $J = 7.6$ Hz, 1H, ArH), 6.82 (d, $J = 8.8$ Hz, 2H, ArH), 4.08 (s, 3H, OCH₃), 3.75 (s, 2H, CH₂), 3.73 (s, 3H, OCH₃); ¹³C NMR (100 MHz, acetone-*d*₆): δ 169.5, 156.7, 133.5, 133.4, 124.9, 123.4, 123.2, 121.7 (2C), 120.4, 120.2, 114.5 (2C), 108.9, 106.7, 66.1, 55.6, 34.5; HR-ESIMS m/z 311.1398 [M + H]⁺ (Calcd for C₁₈H₁₉N₂O₃, 311.1390).

4.1.2.2.18. *N*-(3,4-Dimethylphenyl)-2-(1-methoxy-1*H*-indol-3-yl)acetamide (5r). Four steps yield 26.9%. ¹H NMR (400 MHz, acetone-*d*₆): δ 8.99 (s, 1H, CONH), 7.66 (d, $J = 8.0$ Hz, 1H, ArH), 7.45 (s, 1H, ArH), 7.41 (d, $J = 8.0$ Hz, 1H, ArH), 7.38 (s, 1H, ArH), 7.35 (d, $J = 8.0$ Hz, 1H, ArH), 7.20 (t, $J = 7.6$ Hz, 1H, ArH), 7.06 (t, $J = 7.6$ Hz, 1H, ArH), 6.99 (d, $J = 8.0$ Hz, 1H, ArH), 4.08 (s, 3H, OCH₃), 3.76 (s, 2H, CH₂), 2.16 (m, 6H, CH₃ × 2); ¹³C NMR (100 MHz, acetone-*d*₆): δ 169.6, 138.1, 137.3, 133.4, 132.0, 130.4, 124.9, 123.4, 123.2, 121.4,

120.4, 120.2, 117.7, 108.9, 106.7, 66.1, 34.6, 19.9, 19.1; HR-ESIMS m/z 309.1601 [M + H]⁺ (Calcd for C₁₉H₂₁N₂O₂, 309.1598).

4.1.2.2.19. *N*-(3,5-Dimethylphenyl)-2-(1-methoxy-1*H*-indol-3-yl)acetamide (5s). Four steps yield 29.9%. ¹H NMR (400 MHz, acetone-*d*₆): δ 9.00 (s, 1H, CONH), 7.66 (d, $J = 8.0$ Hz, 1H, ArH), 7.46 (s, 1H, ArH), 7.41 (d, $J = 8.0$ Hz, 1H, ArH), 7.25 (s, 2H, ArH), 7.20 (t, $J = 7.6$ Hz, 1H, ArH), 7.06 (t, $J = 7.6$ Hz, 1H, ArH), 6.66 (s, 1H, ArH), 4.08 (s, 3H, OCH₃), 3.77 (s, 2H, CH₂), 2.20 (s, 6H, CH₃ × 2); ¹³C NMR (100 MHz, acetone-*d*₆): δ 169.7, 140.2, 138.8 (2C), 133.4, 125.7, 124.9, 123.4, 123.2, 120.4, 120.2, 117.9 (2C), 108.9, 106.7, 66.1, 34.7, 21.4 (2C); HR-ESIMS m/z 309.1608 [M + H]⁺ (Calcd for C₁₉H₂₁N₂O₂, 309.1598).

4.1.2.2.20. *N*-(3,5-Dimethoxyphenyl)-2-(1-methoxy-1*H*-indol-3-yl)acetamide (5t). Four steps yield 25.4%. ¹H NMR (400 MHz, acetone-*d*₆): δ 9.19 (s, 1H, CONH), 7.65 (d, $J = 8.0$ Hz, 1H, ArH), 7.44 (s, 1H, ArH), 7.41 (d, $J = 8.0$ Hz, 1H, ArH), 7.21 (t, $J = 7.6$ Hz, 1H, ArH), 7.06 (t, $J = 7.6$ Hz, 1H, ArH), 6.92 (s, 2H, ArH), 6.20 (s, 1H, ArH), 4.07 (s, 3H, OCH₃), 3.78 (s, 2H, CH₂), 3.70 (s, 6H, OCH₃ × 2); ¹³C NMR (100 MHz, acetone-*d*₆): δ 170.0, 161.9 (2C), 141.9, 133.3, 124.8, 123.4, 123.2, 120.4, 120.2, 108.9, 106.5, 98.4 (2C), 96.2, 66.1, 55.4 (2C), 34.7; HR-ESIMS m/z 341.1506 [M + H]⁺ (Calcd for C₁₉H₂₁N₂O₄, 341.1496).

4.1.2.2.21. 2-(1-Methoxy-1*H*-indol-3-yl)-*N*-(3,4,5-trimethoxyphenyl)acetamide (5u). Four steps yield 23.9%. ¹H NMR (400 MHz, acetone-*d*₆): δ 9.12 (s, 1H, CONH), 7.65 (d, $J = 8.0$ Hz, 1H, ArH), 7.45 (s, 1H, ArH), 7.42 (d, $J = 8.0$ Hz, 1H, ArH), 7.21 (t, $J = 7.6$ Hz, 1H, ArH), 7.06 (t, $J = 7.6$ Hz, 1H, ArH), 7.03 (s, 2H, ArH), 4.09 (s, 3H, OCH₃), 3.78 (s, 2H, CH₂), 3.72 (s, 6H, OCH₃ × 2), 3.65 (s, 3H, OCH₃); ¹³C NMR (100 MHz, acetone-*d*₆): δ 169.8, 154.2 (2C), 136.4, 133.4, 124.9, 123.4, 123.2, 120.4, 120.2, 109.0, 106.6, 98.0 (2C), 66.2, 60.5, 56.2 (2C), 34.7; HR-ESIMS m/z 371.1613 [M + H]⁺ (Calcd for C₂₀H₂₃N₂O₅, 371.1601).

4.1.2.2.22. Methyl 2-[3-(1-methoxy-1*H*-indol-3-yl)propanamido]benzoate (5v). Four steps yield 11.7%. ¹H NMR (400 MHz, acetone-*d*₆): δ 10.95 (s, 1H, CONH), 8.72 (d, $J = 8.8$ Hz, 1H, ArH), 7.99 (d, $J = 8.0$ Hz, 1H, ArH), 7.64 (d, $J = 7.6$ Hz, 1H, ArH), 7.58 (t, $J = 7.6$ Hz, 1H, ArH), 7.38 (d, $J = 8.4$ Hz, 1H, ArH), 7.35 (s, 1H, ArH), 7.19 (t, $J = 7.6$ Hz, 1H, ArH), 7.11 (t, $J = 7.6$ Hz, 1H, ArH), 7.05 (t, $J = 7.6$ Hz, 1H, ArH), 4.03 (s, 3H, OCH₃), 3.89 (s, 3H, COOCH₃), 3.15 (t, $J = 7.6$ Hz, 2H, CH₂), 2.83 (t, $J = 7.6$ Hz, 2H, CH₂); ¹³C NMR (100 MHz, acetone-*d*₆): δ 171.6, 169.1, 142.5, 135.2, 133.6, 131.6, 124.7, 123.1 (2C), 122.1, 120.9, 120.2, 119.8, 115.9, 111.9, 109.0, 65.9, 52.8, 39.5, 21.4; HR-ESIMS m/z 353.1508 [M + H]⁺ (Calcd for C₂₀H₂₁N₂O₄, 353.1496).

4.1.2.2.23. Methyl 2-(4-(1-methoxy-1*H*-indol-3-yl)butanamido)benzoate (5w). Four steps yield 9.2%. ¹H NMR (500 MHz, acetone-*d*₆): δ 10.96 (s, 1H, CONH), 8.72 (d, $J = 8.5$ Hz, 1H, ArH), 8.01 (dd, $J = 1.5, 8.0$ Hz, 1H, ArH), 7.59 (m, 2H, ArH), 7.39 (d, $J = 8.0$ Hz, 1H, ArH), 7.32 (s, 1H, ArH), 7.18 (t, $J = 7.5$ Hz, 1H, ArH), 7.12 (t, $J = 7.5$ Hz, 1H, ArH), 7.04 (t, $J = 7.5$ Hz, 1H, ArH), 4.06 (s, 3H, OCH₃), 3.91 (s, 3H, COOCH₃), 2.83 (t, $J = 7.5$ Hz, 2H, CH₂), 2.52 (t, $J = 7.0$ Hz, 2H, CH₂), 2.11 (m, 2H, CH₂); ¹³C NMR (125 MHz, acetone-*d*₆): δ 172.0, 169.2, 142.6, 135.2, 133.8, 131.6, 124.9, 123.0 (2C), 122.1, 120.8, 120.1, 119.9, 115.8, 112.6, 109.0, 65.8, 52.8, 38.3, 26.6, 24.9; HR-ESIMS m/z 367.166 [M + H]⁺ (Calcd for C₂₁H₂₃N₂O₄, 367.1652).

4.1.2.2.24. Methyl 2-(2-(1-ethoxy-1*H*-indol-3-yl)acetamido)benzoate (6a). Four steps yield 24.1%. ¹H NMR (400 MHz, acetone-*d*₆): δ 10.93 (s, 1H, CONH), 8.75 (d, $J = 8.4$ Hz, 1H, ArH), 7.90 (d, $J = 8.4$ Hz, 1H, ArH), 7.56 (m, 3H, ArH), 7.46 (d, $J = 8.4$ Hz, 1H, ArH), 7.21 (t, $J = 7.6$ Hz, 1H, ArH), 7.06 (m, 2H, ArH), 4.43 (m, 2H, OCH₂), 3.87 (s, 2H, CH₂), 3.71 (s, 3H, COOCH₃), 1.43 (t, $J = 6.8$ Hz, 3H, CH₃); ¹³C NMR (100 MHz, acetone-*d*₆): δ 170.2, 168.0, 141.7, 134.4, 133.5, 130.9, 124.4, 124.1, 122.6, 122.5, 120.0, 119.9, 119.1, 115.4, 108.7, 104.2, 74.3, 51.9, 35.1, 13.6; HR-ESIMS m/z 353.1502 [M + H]⁺ (Calcd for C₂₀H₂₁N₂O₄, 353.1496).

4.1.2.2.25. Methyl 2-(2-(1-propoxy-1*H*-indol-3-yl)acetamido)benzoate (6b). Four steps yield 23.8%. ¹H NMR (400 MHz, acetone-*d*₆): δ 10.92 (s, 1H, CONH), 8.75 (d, $J = 8.4$ Hz, 1H, ArH), 7.90 (d,

$J = 8.4$ Hz, 1H, ArH), 7.56 (m, 3H, ArH), 7.46 (d, $J = 8.0$ Hz, 1H, ArH), 7.21 (t, $J = 7.6$ Hz, 1H, ArH), 7.06 (m, 2H, ArH), 4.34 (t, $J = 6.4$ Hz, 2H, OCH₂), 3.87 (s, 2H, CH₂), 3.72 (s, 3H, COOCH₃), 1.86 (m, 2H, CH₂), 1.10 (t, $J = 7.6$ Hz, 3H, CH₃); ¹³C NMR (100 MHz, acetone-*d*₆): δ 170.8, 168.6, 142.3, 135.0, 133.9, 131.5, 124.9, 124.7, 123.2, 123.1, 120.6, 120.5, 119.7, 116.0, 109.2, 104.9, 80.8, 52.5, 35.7, 22.3, 10.6; HR-ESIMS m/z 367.1664 [M + H]⁺ (Calcd for C₂₁H₂₃N₂O₄, 367.1652).

4.1.2.2.26. *N*-(2-Chlorophenyl)-2-(1-ethoxy-1*H*-indol-3-yl)acetamide (**6c**). Four steps yield 25.3%. ¹H NMR (400 MHz, acetone-*d*₆): δ 8.44 (s, 1H, CONH), 8.30 (d, $J = 8.4$ Hz, 1H, ArH), 7.67 (d, $J = 8.0$ Hz, 1H, ArH), 7.60 (s, 1H, ArH), 7.47 (d, $J = 8.0$ Hz, 1H, ArH), 7.32 (d, $J = 8.0$ Hz, 1H, ArH), 7.25 (m, 2H, ArH), 7.09 (t, $J = 7.6$ Hz, 1H, ArH), 7.04 (t, $J = 7.6$ Hz, 1H, ArH), 4.35 (m, 2H, ArH), 3.93 (s, 2H, CH₂), 1.38 (t, $J = 7.2$ Hz, 3H, CH₃); ¹³C NMR (100 MHz, acetone-*d*₆): δ 169.9, 136.0, 134.0, 129.8, 125.5, 124.7, 124.5, 123.4 (2C), 122.8 (2C), 120.7, 119.9, 109.3, 105.4, 74.7, 34.5, 14.1; HR-ESIMS m/z 329.106 [M + H]⁺ (Calcd for C₁₈H₁₈N₂O₂Cl, 329.1051).

4.1.2.2.27. *N*-(2-Chlorophenyl)-2-(1-propoxy-1*H*-indol-3-yl)acetamide (**6d**). Four steps yield 24.9%. ¹H NMR (400 MHz, acetone-*d*₆): δ 8.44 (s, 1H, CONH), 8.30 (d, $J = 8.4$ Hz, 1H, ArH), 7.67 (d, $J = 8.0$ Hz, 1H, ArH), 7.61 (s, 1H, ArH), 7.47 (d, $J = 8.0$ Hz, 1H, ArH), 7.33 (d, $J = 8.0$ Hz, 1H, ArH), 7.26 (m, 2H, ArH), 7.09 (t, $J = 7.6$ Hz, 1H, ArH), 7.04 (t, $J = 7.6$ Hz, 1H, ArH), 4.26 (t, $J = 6.8$ Hz, 2H, OCH₂), 3.92 (s, 2H, CH₂), 1.81 (m, 2H, CH₂), 1.07 (t, $J = 7.6$ Hz, 3H, CH₃); ¹³C NMR (100 MHz, acetone-*d*₆): δ 169.9, 136.1, 133.9, 129.9, 128.3, 125.5 (2C), 124.6, 123.5 (2C), 122.8, 120.7, 119.9, 109.3, 105.5, 80.7, 34.6, 22.3, 10.5; HR-ESIMS m/z 343.1221 [M + H]⁺ (Calcd for C₁₉H₂₀N₂O₂Cl, 343.1208).

4.1.2.2.28. 2-(1-Butoxy-1*H*-indol-3-yl)-*N*-(2-chlorophenyl)acetamide (**6e**). Four steps yield 26.2%. ¹H NMR (400 MHz, acetone-*d*₆): δ 8.43 (s, 1H, CONH), 8.30 (d, $J = 8.4$ Hz, 1H, ArH), 7.66 (d, $J = 8.0$ Hz, 1H, ArH), 7.61 (s, 1H, ArH), 7.46 (d, $J = 8.0$ Hz, 1H, ArH), 7.33 (d, $J = 8.0$ Hz, 1H, ArH), 7.26 (m, 2H, ArH), 7.09 (t, $J = 7.6$ Hz, 1H, ArH), 7.04 (t, $J = 7.6$ Hz, 1H, ArH), 4.30 (t, $J = 6.4$ Hz, 2H, OCH₂), 3.92 (s, 2H, CH₂), 1.78 (m, 2H, CH₂), 1.56 (m, 2H, CH₂), 0.98 (t, $J = 7.2$ Hz, 3H, CH₃); ¹³C NMR (100 MHz, acetone-*d*₆): δ 169.9, 136.1, 133.9, 129.9, 128.4, 125.5 (2C), 124.6, 123.5 (2C), 122.8, 120.7, 120.0, 109.2, 105.5, 79.0, 34.6, 31.0, 19.7, 14.1; HR-ESIMS m/z 357.1373 [M + H]⁺ (Calcd for C₂₀H₂₂N₂O₂Cl, 357.1364).

4.1.2.2.29. *N*-(2-Chlorophenyl)-2-(1-(pentylloxy)-1*H*-indol-3-yl)acetamide (**6f**). Four steps yield 24.7%. ¹H NMR (400 MHz, acetone-*d*₆): δ 8.43 (s, 1H, CONH), 8.30 (d, $J = 8.4$ Hz, 1H, ArH), 7.66 (d, $J = 8.0$ Hz, 1H, ArH), 7.61 (s, 1H, ArH), 7.46 (d, $J = 8.0$ Hz, 1H, ArH), 7.33 (d, $J = 8.0$ Hz, 1H, ArH), 7.26 (m, 2H, ArH), 7.07 (m, 2H, ArH), 4.30 (t, $J = 6.4$ Hz, 2H, OCH₂), 3.92 (s, 2H, CH₂), 1.80 (m, 2H, CH₂), 1.51 (m, 2H, CH₂), 1.41 (m, 2H, CH₂), 0.93 (t, $J = 7.2$ Hz, 3H, CH₃); ¹³C NMR (100 MHz, acetone-*d*₆): δ 169.9, 136.1, 133.9, 129.9, 128.4, 125.5 (2C), 124.6, 123.5 (2C), 122.8, 120.7, 120.0, 109.3, 105.5, 79.3, 34.6, 28.70, 28.68, 23.1, 14.2; HR-ESIMS m/z 371.1528 [M + H]⁺ (Calcd for C₂₁H₂₄N₂O₂Cl, 371.1521).

4.1.2.2.30. *N*-(2-Chlorophenyl)-2-(1-(hexylloxy)-1*H*-indol-3-yl)acetamide (**6g**). Four steps yield 23.0%. ¹H NMR (400 MHz, acetone-*d*₆): δ 8.43 (s, 1H, CONH), 8.30 (d, $J = 8.4$ Hz, 1H, ArH), 7.66 (d, $J = 8.0$ Hz, 1H, ArH), 7.61 (s, 1H, ArH), 7.46 (d, $J = 8.0$ Hz, 1H, ArH), 7.33 (d, $J = 8.0$ Hz, 1H, ArH), 7.26 (m, 2H, ArH), 7.09 (t, $J = 7.6$ Hz, 1H, ArH), 7.04 (t, $J = 7.6$ Hz, 1H, ArH), 4.30 (t, $J = 6.4$ Hz, 2H, OCH₂), 3.92 (s, 2H, CH₂), 1.80 (m, 2H, CH₂), 1.53 (m, 2H, CH₂), 1.35 (m, 4H, CH₂), 0.90 (t, $J = 6.4$ Hz, 3H, CH₃); ¹³C NMR (100 MHz, acetone-*d*₆): δ 169.9, 136.1, 133.9, 129.9, 128.4, 125.5 (2C), 124.6, 123.5 (2C), 122.8, 120.7, 120.0, 109.3, 105.5, 79.3, 34.6, 32.3, 29.0, 26.2, 23.2, 14.2; HR-ESIMS m/z 385.1678 [M + H]⁺ (Calcd for C₂₂H₂₆N₂O₂Cl, 385.1677).

4.1.2.2.31. *N*-(2-Chlorophenyl)-2-(1-(heptyloxy)-1*H*-indol-3-yl)acetamide (**6h**). Four steps yield 24.3%. ¹H NMR (400 MHz, acetone-*d*₆): δ 8.43 (s, 1H, CONH), 8.30 (d, $J = 8.4$ Hz, 1H, ArH), 7.66 (d, $J = 8.0$ Hz, 1H, ArH), 7.61 (s, 1H, ArH), 7.46 (d, $J = 8.0$ Hz, 1H, ArH),

7.33 (d, $J = 8.0$ Hz, 1H, ArH), 7.26 (m, 2H, ArH), 7.07 (m, 2H, ArH), 4.30 (t, $J = 6.4$ Hz, 2H, OCH₂), 3.92 (s, 2H, CH₂), 1.81 (m, 2H, CH₂), 1.53 (m, 2H, CH₂), 1.34 (m, 6H, CH₂), 0.88 (t, $J = 6.0$ Hz, 3H, CH₃); ¹³C NMR (100 MHz, acetone-*d*₆): δ 169.9, 136.1, 133.9, 129.9, 128.4, 125.5 (2C), 124.6, 123.5 (2C), 122.8, 120.7, 120.0, 109.3, 105.5, 79.3, 34.6, 32.4, 29.8, 29.0, 26.5, 23.2, 14.3; HR-ESIMS m/z 399.184 [M + H]⁺ (Calcd for C₂₃H₂₈N₂O₂Cl, 399.1834).

4.1.2.2.32. *N*-(2-Chlorophenyl)-2-(1-(octylloxy)-1*H*-indol-3-yl)acetamide (**6i**). Four steps yield 24.4%. ¹H NMR (400 MHz, acetone-*d*₆): δ 8.43 (s, 1H, CONH), 8.30 (d, $J = 8.4$ Hz, 1H, ArH), 7.66 (d, $J = 8.0$ Hz, 1H, ArH), 7.61 (s, 1H, ArH), 7.46 (d, $J = 8.0$ Hz, 1H, ArH), 7.33 (d, $J = 8.0$ Hz, 1H, ArH), 7.26 (m, 2H, ArH), 7.07 (m, 2H, ArH), 4.31 (t, $J = 6.4$ Hz, 2H, OCH₂), 3.92 (s, 2H, CH₂), 1.81 (m, 2H, CH₂), 1.53 (m, 2H, CH₂), 1.32 (m, 8H, CH₂), 0.88 (t, $J = 6.4$ Hz, 3H, CH₃); ¹³C NMR (100 MHz, acetone-*d*₆): δ 169.9, 136.1, 133.9, 129.9, 128.4, 125.5 (2C), 124.6, 123.5 (2C), 122.8, 120.7, 120.0, 109.3, 105.5, 79.3, 34.6, 32.5, 30.1, 29.9, 29.0, 26.5, 23.3, 14.3; HR-ESIMS m/z 413.1996 [M + H]⁺ (Calcd for C₂₄H₃₀N₂O₂Cl, 413.1990).

4.1.2.2.33. *N*-(2-Chlorophenyl)-2-(1-(nonyloxy)-1*H*-indol-3-yl)acetamide (**6j**). Four steps yield 25.8%. ¹H NMR (400 MHz, acetone-*d*₆): δ 8.43 (s, 1H, CONH), 8.30 (d, $J = 8.4$ Hz, 1H, ArH), 7.66 (d, $J = 8.0$ Hz, 1H, ArH), 7.61 (s, 1H, ArH), 7.46 (d, $J = 8.0$ Hz, 1H, ArH), 7.33 (d, $J = 8.0$ Hz, 1H, ArH), 7.26 (m, 2H, ArH), 7.09 (t, $J = 7.6$ Hz, 1H, ArH), 7.05 (t, $J = 7.6$ Hz, 1H, ArH), 4.30 (t, $J = 6.4$ Hz, 2H, OCH₂), 3.92 (s, 2H, CH₂), 1.80 (m, 2H, CH₂), 1.53 (m, 2H, CH₂), 1.33 (m, 10H, CH₂), 0.87 (t, $J = 6.4$ Hz, 3H, CH₃); ¹³C NMR (100 MHz, acetone-*d*₆): δ 169.9, 136.1, 133.9, 129.9, 128.4, 125.5 (2C), 124.6, 123.5 (2C), 122.7, 120.7, 120.0, 109.3, 105.5, 79.3, 34.6, 32.5, 30.2, 30.1, 29.9, 29.0, 26.5, 23.3, 14.3; HR-ESIMS m/z 427.2158 [M + H]⁺ (Calcd for C₂₅H₃₂N₂O₂Cl, 427.2147).

4.1.2.2.34. *N*-(2-Chlorophenyl)-2-(1-(decylloxy)-1*H*-indol-3-yl)acetamide (**6k**). Four steps yield 26.1%. ¹H NMR (400 MHz, acetone-*d*₆): δ 8.42 (s, 1H, CONH), 8.30 (d, $J = 8.4$ Hz, 1H, ArH), 7.66 (d, $J = 8.0$ Hz, 1H, ArH), 7.61 (s, 1H, ArH), 7.46 (d, $J = 8.0$ Hz, 1H, ArH), 7.33 (d, $J = 8.0$ Hz, 1H, ArH), 7.26 (m, 2H, ArH), 7.07 (m, 2H, ArH), 4.30 (t, $J = 6.4$ Hz, 2H, OCH₂), 3.92 (s, 2H, CH₂), 1.81 (m, 2H, CH₂), 1.53 (m, 2H, CH₂), 1.32 (m, 12H, CH₂), 0.87 (t, $J = 6.4$ Hz, 3H, CH₃); ¹³C NMR (100 MHz, acetone-*d*₆): δ 169.9, 136.1, 133.9, 129.9, 128.4, 125.5 (2C), 124.6, 123.5 (2C), 122.7, 120.7, 120.0, 109.3, 105.5, 79.3, 34.6, 32.6, 30.2 (2C), 30.1, 30.0, 29.0, 26.5, 23.3, 14.3; HR-ESIMS m/z 441.2309 [M + H]⁺ (Calcd for C₂₆H₃₄N₂O₂Cl, 441.2303).

4.1.2.2.35. 2-(1-(Benzylloxy)-1*H*-indol-3-yl)-*N*-(2-chlorophenyl)acetamide (**6l**). Four steps yield 22.9%. ¹H NMR (300 MHz, acetone-*d*₆): δ 8.43 (s, 1H, CONH), 8.31 (dd, $J = 1.2, 8.4$ Hz, 1H, ArH), 7.35 (m, 6H, ArH), 7.07 (m, 2H, ArH), 5.28 (2H, s, CH₂), 3.90 (s, 2H, CH₂); ¹³C NMR (75 MHz, acetone-*d*₆): δ 169.9, 136.0, 135.8, 134.0, 130.5 (2C), 129.81, 129.78, 129.7, 129.3 (2C), 128.3, 125.5, 124.8, 124.5, 123.4, 122.9, 120.7, 119.9, 109.4, 105.5, 80.9, 34.5; HR-ESIMS m/z 391.1215 [M + H]⁺ (Calcd for C₂₃H₂₀N₂O₂Cl, 391.1208).

4.1.2.2.36. *N*-(2-Chlorophenyl)-2-(1-phenethoxy-1*H*-indol-3-yl)acetamide (**6m**). Four steps yield 22.6%. ¹H NMR (400 MHz, acetone-*d*₆): δ 8.43 (s, 1H, CONH), 8.28 (d, $J = 8.4$ Hz, 1H, ArH), 7.65 (d, $J = 8.0$ Hz, 1H, ArH), 7.57 (s, 1H, ArH), 7.31 (m, 8H, ArH), 7.18 (t, 1H, ArH), 7.06 (m, 2H, ArH), 4.54 (t, $J = 6.8$ Hz, 2H, CH₂), 3.91 (s, 2H, CH₂), 3.14 (t, $J = 6.8$ Hz, 2H, CH₂); ¹³C NMR (100 MHz, acetone-*d*₆): δ 169.9, 138.8, 136.1, 133.9, 129.9 (2C), 129.8, 129.3 (2C), 128.4, 127.4, 125.5, 124.61, 124.58, 123.5, 122.9 (2C), 120.8, 119.9, 109.3, 105.7, 79.7, 35.3, 34.5; HR-ESIMS m/z 405.1345 [M + H]⁺ (Calcd for C₂₄H₂₂N₂O₂Cl, 405.1364).

4.1.2.2.37. *N*-(2-Chlorophenyl)-2-{1-[(4-methoxybenzyl)oxy]-1*H*-indol-3-yl}acetamide (**6n**). Four steps yield 28.9%. ¹H NMR (400 MHz, acetone-*d*₆): δ 8.39 (s, 1H, CONH), 8.28 (d, $J = 8.0$ Hz, 1H, ArH), 7.65 (d, $J = 8.0$ Hz, 1H, ArH), 7.42 (m, 4H, ArH), 7.34 (d, $J = 8.0$ Hz, 1H, ArH), 7.28 (t, $J = 8.0$ Hz, 1H, ArH), 7.20 (t, $J = 7.6$ Hz, 1H, ArH), 7.07 (m, 2H, ArH), 6.91 (d, $J = 8.4$ Hz, 2H, ArH), 5.22 (s, 2H,

CH₂), 3.88 (s, 2H, CH₂), 3.76 (s, 3H, OCH₃); ¹³C NMR (100 MHz, acetone-*d*₆): δ 169.9, 161.3, 136.1, 134.0, 132.3 (2C), 129.9, 128.3, 127.9, 125.5, 125.0, 124.6 (2C), 123.4, 122.9, 120.7, 119.9, 114.7 (2C), 109.5, 105.4, 80.6, 55.5, 34.5; HR-ESIMS *m/z* 421.1312 [M + H]⁺ (Calcd for C₂₄H₂₂N₂O₃Cl, 421.1313).

4.1.2.2.38. 3-(2-((2-Chlorophenyl)amino)-2-oxoethyl)-1H-indol-1-yl acetate (**6o**). Four steps yield 23.4%. ¹H NMR (400 MHz, acetone-*d*₆): δ 8.52 (s, 1H, CONH), 8.28 (d, *J* = 8.0 Hz, 1H, ArH), 7.69 (d, *J* = 8.4 Hz, 1H, ArH), 7.51 (s, 1H, ArH), 7.34 (d, *J* = 8.4 Hz, 2H, ArH), 7.26 (m, 2H, ArH), 7.14 (t, *J* = 7.6 Hz, 1H, ArH), 7.06 (t, *J* = 7.6 Hz, 1H, ArH), 3.95 (s, 2H, CH₂), 2.42 (s, 3H, COCH₃); ¹³C NMR (100 MHz, acetone-*d*₆): δ 169.7, 169.4, 136.1, 135.3, 129.9, 128.3, 125.8, 125.6, 125.1, 124.0, 123.0, 121.3, 120.0, 109.4, 107.4, 34.4, 18.0; HR-ESIMS *m/z* 343.0838 [M + H]⁺ (Calcd for C₁₈H₁₆N₂O₃Cl, 343.0844).

4.1.2.2.39. 3-(2-((2-Chlorophenyl)amino)-2-oxoethyl)-1H-indol-1-yl benzoate (**6p**). Four steps yield 21.9%. ¹H NMR (400 MHz, acetone-*d*₆): δ 8.60 (s, 1H, CONH), 8.29 (d, *J* = 8.0 Hz, 1H, ArH), 8.240 (d, *J* = 7.6 Hz, 2H, ArH), 7.81 (t, *J* = 7.2 Hz, 1H, ArH), 7.75 (d, *J* = 8.0 Hz, 1H, ArH), 7.66 (m, 3H, ArH), 7.38 (m, 2H, ArH), 7.28 (m, 2H, ArH), 7.18 (t, *J* = 7.6 Hz, 1H, ArH), 7.07 (t, *J* = 7.6 Hz, 1H, ArH), 4.01 (s, 2H, CH₂); ¹³C NMR (100 MHz, acetone-*d*₆): δ 169.7, 165.3, 136.1, 135.8, 135.6, 130.9 (2C), 130.0 (2C), 129.9, 128.3, 127.4, 126.3, 125.6, 125.4, 124.2, 123.1 (2C), 121.6, 120.2, 109.6, 108.0, 34.4; HR-ESIMS *m/z* 405.1010 [M + H]⁺ (Calcd for C₂₃H₁₈N₂O₃Cl, 405.1000).

4.1.2.2.40. 2-(1-Propoxy-1H-indol-3-yl)-N-(2-(trifluoromethyl)phenyl)acetamide (**6q**). Four steps yield 4.2%. ¹H NMR (400 MHz, acetone-*d*₆): δ 8.30 (s, 1H, CONH), 8.11 (d, *J* = 8.4 Hz, 1H, ArH), 7.61 (m, 4H, ArH), 7.46 (d, *J* = 8.4 Hz, 1H, ArH), 7.29 (t, *J* = 7.6 Hz, 1H, ArH), 7.24 (t, *J* = 7.6 Hz, 1H, ArH), 7.09 (t, *J* = 7.6 Hz, 1H, ArH), 4.26 (t, *J* = 6.8 Hz, 2H, CH₂), 3.90 (s, 2H, CH₂), 1.83 (m, 2H, CH₂), 1.08 (t, *J* = 7.6 Hz, 3H, CH₃); ¹³C NMR (150 MHz, acetone-*d*₆): δ 170.2, 136.8, 133.9, 133.7, 126.8 (q, C-CF₃), 126.2, 125.7, 125.6, 125.5, 124.6, 123.9, 123.4, 120.7, 119.8, 109.2, 105.2, 80.8, 34.3, 22.3, 10.5; HR-ESIMS *m/z* 377.1477 [M + H]⁺ (Calcd for C₂₀H₂₀N₂O₂F₃, 377.1471).

4.1.2.2.41. 2-(1-Methoxy-1H-indol-3-yl)-N-(pyridin-2-yl)acetamide (**10a**). Four steps yield 10.3%. ¹H NMR (300 MHz, acetone-*d*₆): δ 9.36 (s, 1H, CONH), 8.22 (m, 2H, ArH), 7.70 (m, 2H, ArH), 7.52 (s, 1H, ArH), 7.43 (d, *J* = 7.8 Hz, 1H, ArH), 7.22 (t, *J* = 7.5 Hz, 1H, ArH), 7.08 (t, *J* = 7.5 Hz, 1H, ArH), 7.01 (dd, *J* = 4.5, 7.2 Hz, 1H, ArH), 4.07 (s, 3H, OCH₃), 3.93 (s, 2H, CH₂); ¹³C NMR (75 MHz, acetone-*d*₆): δ 170.5, 153.1, 148.7, 138.7, 133.3, 124.8, 123.6, 123.3, 120.5, 120.2, 120.1, 114.1, 109.0, 106.1, 66.2, 34.5; HR-ESIMS *m/z* 282.1239 [M + H]⁺ (Calcd for C₁₆H₁₆N₃O₂, 282.1237).

4.1.2.2.42. 2-(1-Methoxy-1H-indol-3-yl)-N-(pyridin-3-yl)acetamide (**10b**). Four steps yield 9.3%. ¹H NMR (400 MHz, acetone-*d*₆): δ 9.42 (s, 1H, CONH), 8.73 (s, 1H, ArH), 8.24 (d, *J* = 4.4 Hz, 1H, ArH), 8.12 (dd, *J* = 1.6, 8.4 Hz, 1H, ArH), 7.65 (d, *J* = 8.0 Hz, 1H, ArH), 7.48 (s, 1H, ArH), 7.42 (d, *J* = 8.0 Hz, 1H, ArH), 7.24 (m, 2H, ArH), 7.07 (t, 7.6 Hz, 1H, ArH), 4.08 (s, 3H, OCH₃), 3.84 (s, 2H, CH₂); ¹³C NMR (100 MHz, acetone-*d*₆): δ 170.5, 145.2, 141.9, 136.9, 133.3, 127.0, 124.8, 124.2, 123.5, 123.2, 120.5, 120.1, 109.0, 106.1, 66.2, 34.4; HR-ESIMS *m/z* 282.1242 [M + H]⁺ (Calcd for C₁₆H₁₆N₃O₂, 282.1237).

4.1.2.2.43. 2-(1-Methoxy-1H-indol-3-yl)-N-(pyridin-4-yl)acetamide (**10c**). Four steps yield 10.0%. ¹H NMR (400 MHz, acetone-*d*₆): δ 9.59 (s, 1H, CONH), 8.39 (d, *J* = 5.6 Hz, 2H, ArH), 7.60 (m, 3H, ArH), 7.47 (s, 1H, ArH), 7.42 (d, *J* = 8.0 Hz, 1H, ArH), 7.21 (t, *J* = 7.6 Hz, 1H, ArH), 7.06 (t, *J* = 7.6 Hz, 1H, ArH), 4.09 (s, 3H, OCH₃), 3.84 (s, 2H, CH₂); ¹³C NMR (100 MHz, acetone-*d*₆): δ 171.0, 151.2 (2C), 146.9, 133.3, 124.8, 123.5, 123.2, 120.5, 120.1, 114.1 (2C), 109.0, 105.8, 66.2, 34.7; HR-ESIMS *m/z* 282.1243 [M + H]⁺ (Calcd for C₁₆H₁₆N₃O₂, 282.1237).

4.1.2.2.44. N-(3-Chloropyridin-4-yl)-2-(1-methoxy-1H-indol-3-yl)acetamide (**10d**). Four steps yield 15.8%. ¹H NMR (400 MHz, acetone-*d*₆): δ 8.69 (s, 1H, CONH), 8.42 (s, 1H, ArH), 8.36 (m, 2H, ArH), 7.66 (d, *J* = 8.0 Hz, 1H, ArH), 7.63 (s, 1H, ArH), 7.47 (d,

J = 8.0 Hz, 1H, ArH), 7.25 (t, *J* = 7.6 Hz, 1H, ArH), 7.10 (t, *J* = 7.6 Hz, 1H, ArH), 4.12 (s, 3H, OCH₃), 4.01 (s, 2H, CH₂); ¹³C NMR (100 MHz, acetone-*d*₆): δ 170.9, 149.9, 149.8, 142.5, 133.3, 124.5, 123.9, 123.6, 120.9, 120.2, 119.9, 115.1, 109.2, 105.2, 66.4, 34.6; HR-ESIMS *m/z* 316.086 [M + H]⁺ (Calcd for C₁₆H₁₅N₃O₂Cl, 316.0847).

4.1.2.2.45. N-(3-Bromopyridin-4-yl)-2-(1-methoxy-1H-indol-3-yl)acetamide (**10e**). Four steps yield 16.9%. ¹H NMR (400 MHz, acetone-*d*₆): δ 8.51 (s, 1H, CONH), 8.38 (d, *J* = 5.6 Hz, 1H, ArH), 8.33 (d, *J* = 5.6 Hz, 1H, ArH), 7.65 (m, 2H, ArH), 7.48 (d, *J* = 8.0 Hz, 1H, ArH), 7.26 (t, *J* = 7.6 Hz, 1H, ArH), 7.11 (t, *J* = 7.6 Hz, 1H, ArH), 4.14 (s, 3H, OCH₃), 3.99 (s, 2H, CH₂); ¹³C NMR (100 MHz, acetone-*d*₆): δ 170.8, 152.5, 150.3, 143.5, 133.4, 124.5, 124.1, 123.7, 121.0, 119.9, 115.3, 110.9, 109.2, 104.9, 66.5, 34.7; HR-ESIMS *m/z* 360.0345 [M + H]⁺ (Calcd for C₁₆H₁₅N₃O₂Br, 360.0342).

4.1.2.2.46. N-(3-Chloropyridin-4-yl)-2-(1-propoxy-1H-indol-3-yl)acetamide (**10f**). Four steps yield 21.6%. ¹H NMR (400 MHz, acetone-*d*₆): δ 8.66 (s, 1H, CONH), 8.42 (s, 1H, ArH), 8.36 (m, 2H, ArH), 7.65 (d, *J* = 8.0 Hz, 1H, ArH), 7.63 (s, 1H, ArH), 7.47 (d, *J* = 8.0 Hz, 1H, ArH), 7.24 (t, *J* = 7.6 Hz, 1H, ArH), 7.10 (t, *J* = 7.6 Hz, 1H, ArH), 4.26 (t, *J* = 6.8 Hz, 2H, CH₂), 4.00 (s, 2H, CH₂), 1.81 (m, 2H, CH₂), 1.08 (t, 3H, CH₃); ¹³C NMR (100 MHz, acetone-*d*₆): δ 170.9, 149.9, 149.8, 142.5, 133.8, 124.7, 124.5, 123.5, 120.8, 119.9, 115.0, 114.9, 109.3, 104.9, 80.8, 34.7, 22.3, 10.5; HR-ESIMS *m/z* 344.1166 [M + H]⁺ (Calcd for C₁₈H₁₉N₃O₂Cl, 344.1160).

4.1.2.2.47. N-(3-Fluoropyridin-4-yl)-2-(1-propoxy-1H-indol-3-yl)acetamide (**10g**). Four steps yield 10.3%. ¹H NMR (400 MHz, acetone-*d*₆): δ 9.29 (s, 1H, CONH), 8.36 (m, 2H, ArH), 8.28 (d, *J* = 6.4 Hz, 1H, ArH), 7.65 (d, *J* = 8.0 Hz, 1H, ArH), 7.52 (s, 1H, ArH), 7.43 (d, *J* = 7.6 Hz, 1H, ArH), 7.21 (t, *J* = 7.6 Hz, 1H, ArH), 7.07 (t, *J* = 7.6 Hz, 1H, ArH), 4.24 (t, *J* = 6.4 Hz, 2H, CH₂), 3.98 (s, 2H, CH₂), 1.79 (m, 2H, CH₂), 1.07 (t, 3H, CH₃); ¹³C NMR (100 MHz, acetone-*d*₆): δ 171.1, 147.45, 147.39, 138.0, 137.8, 133.8, 124.7, 124.3, 123.3, 120.5, 120.0, 115.6, 110.6, 109.2, 105.4, 80.6, 34.4, 22.3, 10.5; HR-ESIMS *m/z* 328.1458 [M + H]⁺ (Calcd for C₁₈H₁₈N₃O₂F, 328.1456).

4.1.2.2.48. 2-(1-Propoxy-1H-indol-3-yl)-N-(pyrimidin-4-yl)acetamide (**10h**). Four steps yield 7.2%. ¹H NMR (400 MHz, acetone-*d*₆): δ 9.73 (s, 1H, CONH), 8.75 (s, 1H, CONH), 8.59 (d, *J* = 5.6 Hz, 1H, ArH), 8.13 (d, *J* = 5.6 Hz, 1H, ArH), 7.67 (d, *J* = 8.0 Hz, 1H, ArH), 7.53 (s, 1H, ArH), 7.43 (d, *J* = 8.0 Hz, 1H, ArH), 7.21 (t, *J* = 7.6 Hz, 1H, ArH), 7.07 (t, *J* = 6.4 Hz, 1H, ArH), 4.23 (t, *J* = 6.4 Hz, 2H, CH₂), 3.98 (s, 2H, CH₂), 1.79 (m, 2H, CH₂), 1.06 (t, *J* = 7.6 Hz, 3H, CH₃); ¹³C NMR (100 MHz, acetone-*d*₆): δ 171.8, 159.2, 159.0, 158.6, 133.8, 124.7, 124.4, 123.2, 120.5, 120.1, 110.5, 109.2, 105.2, 80.6, 34.5, 22.3, 10.5; HR-ESIMS *m/z* 311.1513 [M + H]⁺ (Calcd for C₁₇H₁₉N₄O₂, 311.1503).

4.1.2.2.49. 2-(1-Butoxy-1H-indol-3-yl)-N-(3-chloropyridin-4-yl)acetamide (**10i**). Four steps yield 20.5%. ¹H NMR (400 MHz, acetone-*d*₆): δ 8.66 (s, 1H, CONH), 8.42 (s, 1H, ArH), 8.36 (m, 2H, ArH), 7.64 (m, 2H, ArH), 7.47 (d, *J* = 8.4 Hz, 1H, ArH), 7.25 (t, *J* = 7.6 Hz, 1H, ArH), 7.10 (t, *J* = 7.6 Hz, 1H, ArH), 4.31 (t, *J* = 7.2 Hz, 2H, CH₂), 4.00 (s, 2H, CH₂), 1.78 (m, 2H, CH₂), 1.54 (m, 2H, CH₂), 0.98 (t, *J* = 7.6 Hz, 3H, CH₃); ¹³C NMR (100 MHz, acetone-*d*₆): δ 170.9, 149.9, 149.8, 142.5, 133.9, 124.7, 124.5, 123.6, 120.8, 119.9, 115.03, 114.96, 109.3, 104.9, 79.1, 34.7, 31.0, 19.7, 14.1; HR-ESIMS *m/z* 358.1321 [M + H]⁺ (Calcd for C₁₉H₂₁N₃O₂Cl, 358.1317).

4.1.2.2.50. N-(3-Chloropyridin-4-yl)-2-(1-pentyloxy-1H-indol-3-yl)acetamide (**10j**). Four steps yield 20.2%. ¹H NMR (400 MHz, acetone-*d*₆): δ 8.66 (s, 1H, CONH), 8.42 (s, 1H, ArH), 8.36 (m, 2H, ArH), 7.64 (m, 2H, ArH), 7.47 (d, *J* = 8.4 Hz, 1H, ArH), 7.25 (t, *J* = 7.6 Hz, 1H, ArH), 7.10 (t, *J* = 7.6 Hz, 1H, ArH), 4.31 (t, *J* = 7.2 Hz, 2H, CH₂), 4.00 (s, 2H, CH₂), 1.81 (m, 2H, CH₂), 1.50 (m, 2H, CH₂), 1.40 (m, 2H, CH₂), 0.93 (t, *J* = 7.2 Hz, 3H, CH₃); ¹³C NMR (100 MHz, acetone-*d*₆): δ 170.9, 149.9, 149.8, 142.5, 133.9, 124.7, 124.5, 123.6, 120.8, 119.9, 115.0, 109.3, 104.9, 79.4, 34.7, 28.69, 28.68, 23.1, 14.2; HR-ESIMS *m/z* 372.1484 [M + H]⁺ (Calcd for C₂₀H₂₃N₃O₂Cl, 372.1473).

4.1.2.3. Synthesis of 14 and 15. To a cold solution of **11** in MeOH (0 °C) was added sodium tungstate dehydrate (0.3 equiv.) and dropwise hydrogen peroxide (30%, 10 equiv.), stirred at 10–15 °C for 1 h, then added CH₂Cl₂ and water and stirred for 10 min. After separation, washed with brine, and dried over anhydrous Na₂SO₄, the organic phase was evaporated to give a residue; then added DMF, K₂CO₃ (3 equiv.), and the alkyl halide (1.5 equiv.), stirred at room temperature for 2 h, and followed by addition of water and ethyl acetate then stirring for 10 min. The organic layer was separated, dried over anhydrous Na₂SO₄, and evaporated to give a residue. The residue was dissolved in diethyl ether, added oxalyl chloride (1.5 equiv.) dropwise at 0 °C, and stirred at room temperature for 2 h. After removal of the diethyl ether and redissolving in CH₂Cl₂, to the solution was added 4-amino-3-chloropyridine (1.2 equiv.) and triethylamine (2.0 equiv.) dropwise at 0 °C then stirred at room temperature for 3 h. Evaporation of the solvent gave a residue that was purified by silica gel column chromatography (petroleum ether/ethyl acetate 1:1) to furnish **14**. To a solution of **14** (1 equiv.) in methanol was added sodium borohydride (3.0 equiv.), stirred for 1 h, then diluted with water and extracted with ethyl acetate. The ethyl acetate layer was washed with brine then evaporated to afford a residue, which was purified by silica gel column chromatography (petroleum ether/ethyl acetate 1:1) to obtain **15**.

4.1.2.3.1. N-(3-Chloropyridin-4-yl)-2-oxo-2-(1-propoxy-1H-indol-3-yl)acetamide (14). Three steps yield 45.7%. ¹H NMR (400 MHz, acetone-d₆): δ 10.11 (s, 1H, CONH), 9.16 (s, 1H, ArH), 8.63 (s, 1H, ArH), 8.53 (d, J = 5.6 Hz, 1H, ArH), 8.48 (d, J = 5.6 Hz, 1H, ArH), 8.41 (d, J = 7.2 Hz, 1H, ArH), 7.65 (d, J = 8.0 Hz, 1H, ArH), 7.41 (m, 1H, ArH), 4.49 (t, J = 6.4 Hz, 2H, CH₂), 1.90 (m, 2H, CH₂), 1.13 (t, J = 7.2 Hz, 3H, CH₃); ¹³C NMR (150 MHz, DMSO-d₆): δ 178.5, 160.9, 149.5, 149.1, 140.5, 135.7, 132.2, 124.8, 124.2, 123.1, 121.71, 121.66, 115.8, 109.7, 106.4, 81.2, 21.0, 10.0; HR-ESIMS m/z 358.0971 [M + H]⁺ (Calcd for C₁₈H₁₇N₃O₃Cl, 358.0953).

4.1.2.3.2. N-(3-Chloropyridin-4-yl)-2-hydroxy-2-(1-propoxy-1H-indol-3-yl)acetamide (15). Yield 79%. ¹H NMR (400 MHz, DMSO-d₆): δ 9.93 (s, 1H, CONH), 8.65 (s, 1H, ArH), 8.44 (d, J = 5.2 Hz, 1H, ArH), 8.26 (d, J = 5.6 Hz, 1H, ArH), 7.71 (s, 1H, ArH), 7.67 (d, J = 8.0 Hz, 1H, ArH), 7.43 (d, J = 8.4 Hz, 1H, ArH), 7.20 (t, J = 7.6 Hz, 1H, ArH), 7.06 (t, J = 7.6 Hz, 1H, ArH), 6.98 (d, J = 3.6 Hz, 1H, OH), 5.48 (d, J = 4.0 Hz, 1H, CH), 4.19 (t, J = 6.8 Hz, 2H, CH₂), 1.72 (m, 2H, CH₂), 1.01 (t, J = 7.2 Hz, 3H, CH₃); ¹³C NMR (100 MHz, DMSO-d₆): δ 171.8, 149.21, 149.16, 140.7, 132.4, 123.6, 122.4, 121.7, 119.9 (2C), 119.8, 114.1, 110.0, 108.4, 79.7, 68.1, 21.1, 10.1; HR-ESIMS m/z 360.1115 [M + H]⁺ (Calcd for C₁₈H₁₉N₃O₃Cl, 360.1109).

4.1.2.4. General procedure for the synthesis of 20. To a solution of **16** (1.0 mmol, 1 equiv.) and a derivative of pyridine formaldehyde (1.1 equiv.) in 2 mL of MeOH was added an aqueous solution of sodium hydroxide (4 M, 2 equiv.) at 0–5 °C in 10 min, and stirred at room temperature for 2 h. The formed precipitates were collected by filtration, washed with MeOH, and dried under vacuum to afford the intermediate **17** as a pale yellow solid. Subsequently **20** was synthesized from the intermediate **17** following the same reduction, N-oxidation, and alkylation as described for the synthesis of **5**, **6**, and **10**.

4.1.2.4.1. 1-Propoxy-3-(pyridin-4-ylmethyl)-1H-indole (20a). Four steps yield 33.8%. ¹H NMR (400 MHz, acetone-d₆): δ 8.47 (d, J = 5.2 Hz, 2H, ArH), 7.45 (m, 2H, ArH), 7.37 (s, 1H, ArH), 7.31 (d, 2H, ArH), 7.20 (t, J = 7.6 Hz, 1H, ArH), 7.02 (t, J = 7.6 Hz, 1H, ArH), 4.22 (t, J = 6.4 Hz, 2H, CH₂), 4.11 (s, 2H, CH₂), 1.79 (m, 2H, CH₂), 1.07 (t, J = 7.6 Hz, 3H, CH₃); ¹³C NMR (100 MHz, acetone-d₆): δ 151.7, 150.3 (2C), 134.1, 124.9 (2C), 124.4, 123.7, 123.2, 120.3, 119.9, 109.9, 109.2, 80.5, 31.1, 22.3, 10.5; HR-ESIMS m/z 267.1498 [M + H]⁺ (Calcd for C₁₈H₁₉N₂O, 267.1492).

4.1.2.4.2. 3-[(3-Chloropyridin-4-yl)methyl]-1-propoxy-1H-indole (20b). Four steps yield 29.3%. ¹H NMR (400 MHz, acetone-d₆): δ 8.53 (s, 1H, ArH), 8.34 (d, J = 4.4 Hz, 1H, ArH), 7.49 (d, J = 7.6 Hz, 1H, ArH), 7.44 (d, J = 8.0 Hz, 1H, ArH), 7.37 (s, 1H, ArH), 7.21 (m, 2H, ArH), 7.04 (t, J = 7.6 Hz, 1H, ArH), 4.23 (m, 4H, CH₂ × 2), 1.79 (m, 2H, CH₂), 1.06 (t, J = 7.2 Hz, 3H, CH₃); ¹³C NMR (100 MHz, acetone-d₆): δ 149.8, 148.9 (2C), 148.2, 134.0, 126.0, 124.4, 124.2, 123.3, 120.5, 119.8, 109.3, 108.1, 80.6, 28.6, 22.3, 10.5; HR-ESIMS m/z 301.1116 [M + H]⁺ (Calcd for C₁₇H₁₈N₂OCl, 301.1102).

4.1.2.4.3. 3-[(3,5-Dichloropyridin-4-yl)methyl]-1-propoxy-1H-indole (20c). Four steps yield 23.7%. ¹H NMR (400 MHz, acetone-d₆): δ 8.53 (s, 2H, ArH), 7.69 (d, J = 8.0 Hz, 1H, ArH), 7.41 (d, J = 8.0 Hz, 1H, ArH), 7.21 (t, J = 7.6 Hz, 1H, ArH), 7.09 (m, 2H, ArH), 4.36 (s, 2H, CH₂), 4.15 (t, J = 6.4 Hz, 2H, CH₂), 1.72 (m, 2H, CH₂), 1.00 (t, J = 7.6 Hz, 3H, CH₃); ¹³C NMR (125 MHz, acetone-d₆): δ 148.6 (2C), 145.9, 133.9, 133.6 (2C), 124.3, 123.4, 123.3, 120.5, 119.8, 109.2, 107.0, 80.5, 27.2, 22.2, 10.5; HR-ESIMS m/z 335.0717 [M + H]⁺ (Calcd for C₁₇H₁₇N₂OCl₂, 335.0712).

4.2. Biology

4.2.1. Cells and plasmids

HEK 293T cells were from the China Infrastructure of Cell Line Resource (Beijing, China) and cultured in Dulbecco's modified Eagle's medium containing 10% FBS, 100 IU/mL penicillin, and 100 µg/mL streptomycin at 37 °C under 5% CO₂. The pNL4-3.luc.R⁻E⁻ plasmid was acquired from the National Institute of Health AIDS Research and Reference Reagent Program. Vesicular stomatitis virus glycoprotein (VSVG) plasmid was kindly provided by Dr. Lijun Rong (University of Illinois at Chicago). The pNL4-3.luc.R⁻E⁻ plasmids with RT mutations (pNL4-3.luc.R⁻E⁻RT-mutant) were constructed as described previously [56].

4.2.2. Anti-HIV-1 activity assay by pseudoviruses

VSVG plasmid and env-deficient HIV vector containing luciferase reporter (pNL4-3.luc.R⁻E⁻ or pNL4-3.luc.R⁻E⁻RT-mutant) were co-transfected into HEK 293T cells. 48 h post transfection, the supernatant was collected and filtered through 0.45 µm filters, the harvested VSVG/HIV-1 or VSVG/HIV-1RT-mutant virions were quantified by using an ELISA kit (ZeptoMetrix, Cat. 0801111). HEK 293T cells were seeded on 48-well plates at a density of 3 × 10⁴ cells/well one day prior to infection. The tested compounds were added to wells 15 min ahead of VSVG/HIV-1 or VSVG/HIV-1RT-mutant infection (0.1 ng p24/well). The infected cells were lysed 48 h postinfection, and the luciferase activity was measured using a Sirius luminometer (Berthold Detection System) according to the manufacturer's instructions. Infectivity (%) = luciferase activity_{tested compound}/luciferase activity_{DMSO} × 100 [56].

4.2.3. Cell viability assay

HEK 293T cells, 4 × 10³ cells/well in a 96-well plate, were treated with the compounds at the indicated concentration for 48 h. The cell viability was measured by the CellTiter-Glo® Assay (Promega, Madison, WI, USA) according to the manufacturer's protocol. Cells treated with the same amount DMSO (1%) served as the solvent control. The cell viability of the each tested compound was calculated as Cell viability (%) = RLUs_{tested compound}/RLUs_{DMSO} × 100% [74].

4.2.4. Time-of-drug addition (TOA) assay

HEK 293T cells were seeded in 48-well plates one day before infection. The tested compounds and reference drugs were added into the different wells at the time points of 0, 2, 4, 6, 8, 10, 12, 14, 16 h of VSVG/HIV-1 infection. The final concentrations for **6d**, **10f**, **10i** and reference drugs AZT, EFV, RAL were 3 µM, 0.5 µM, 0.3 µM,

1 μ M, 1 μ M, and 1 μ M respectively. The luciferase activity of cell lysate was measured 48 h postinfection [75].

4.2.5. RT RNA-Dependent DNA polymerase activity detection

HIV-1 reverse transcriptase RNA-dependent DNA polymerase activity was detected as described previously [59]. The tested compound was added into 60 μ L reaction system containing 11.7 μ g/mL poly(rA), 1.125 μ g/mL oligo(dT)15, 2.8 μ M dTTP, 800 nM Digoxigenin-11-dUTP, 40 nM Biotin-11-dUTP, 50 mM Tris-HCl (pH 7.8), 290 mM KCl, 30 mM MgCl₂ and 10 mM DTT. The reaction was initiated by RT addition. Blank control was conducted without adding RT, while solvent control was to add DMSO instead of the tested compound. The mixture was incubated at 37 °C for 1 h followed by being transferred into a streptavidin-coated plate (Roche) for 1 h incubation at 37 °C. The supernatant was then discarded and the plate was washed with PBS. Anti-DIG-POD was added to the plate and incubated at 37 °C for 1 h. The plate was washed and TMB (3,3',5,5'-tetramethylbenzidine) was added. After 15 min, 1 M H₂SO₄ was added to terminate the reaction, and the OD₄₅₀ values were read by a multimode reader (Tecan). RNA-Dependent DNA polymerase activity = $(A_{450} \text{ tested compound} - A_{450} \text{ blank control}) / (A_{450} \text{ solvent control} - A_{450} \text{ blank control}) \times 100\%$.

4.2.6. Ribonuclease H activity detection

Detection of Ribonuclease H activity was performed as described previously [60]. Briefly, the 1 μ L tested compound was added into 49 μ L reaction system which containing 50 mM Tris-HCl (pH 8.0), 60 mM KCl, 10 mM MgCl₂, and RT. Then 50 μ L RNA/DNA substrate solution containing 50 mM Tris-HCl (pH 8.0), 60 mM KCl and 4.5 μ M RNA/DNA substrate (TriLink Biotechnologies) were added into the reaction system to react for 30 min at room temperature. Blank control was conducted without adding RT, while solvent control was to add DMSO instead of the tested compound. The reaction was terminated by adding 50 μ L 0.5 M EDTA. The relative fluorescence units (RFU) were detected by multimode reader (Tecan) (Ex = 490 nm, Em = 528 nm). Ribonuclease H activity = $(\text{RFU}_{\text{tested compound}} - \text{RFU}_{\text{blank control}}) / (\text{RFU}_{\text{solvent control}} - \text{RFU}_{\text{blank control}}) \times 100\%$.

4.2.7. Statistical analysis

Mean value, standard deviation (SD), half maximal effective concentration (EC₅₀), half maximal inhibitory concentration (IC₅₀) and 50% cytotoxic concentration (CC₅₀) were calculated by Graph-Pad Prism software.

4.3. Molecular docking

The molecular docking was performed with the Discovery Studio Client v18.1.0.17334 software package (Accelrys, San Diego, USA). The complex structure was obtained from the Protein Data Bank (WT RT: 1TL1, Y181C RT: 1JLB, K103N–Y181C double-mutated RT: 5VQY, L100I–K103N double-mutated RT: 2ZE2). In the complex, water molecules and the original ligand were removed, and the binding cavity of active site was re-docked with the compound to be tested, both the structures of receptor and ligand for docking were energy optimized. The docking was carried out with the CDocker protocol that employs CHARMM. All calculations were performed on a DELL OptiPlex 7040 workstation.

Declaration of competing interest

The authors declare that they have no known competing financial interests or personal relationships that could have appeared to influence the work reported in this paper.

Acknowledgments

Financial support of the National Natural Science Foundation of China (81630094 and 81473256), CAMS Innovation Fund for Medical Science of China (2017-I2M-3-010 and 2016-I2M-1-014), the Science and Technology Program of Beijing (Z151100000115008), and the Drug Innovation Major Project of China (2018ZX09711001-004-004, 2018ZX09711001-003-002, and 2015ZX09102-023) is acknowledged.

Appendix A. Supplementary data

Supplementary data to this article can be found online at <https://doi.org/10.1016/j.ejmech.2020.112071>.

Abbreviations

AIDS	acquired immunodeficiency syndrome
Anti-DIG-POD	anti-digoxigenin peroxidase
AZT	zidovudine
CC	column chromatography
CC ₅₀	50% cytotoxic concentration
DMAP	4-dimethylaminopyridine
DMF	N,N-dimethylformamide
DMSO	dimethyl sulfoxide
EC ₅₀	half maximal effective concentration
EDCI	N-(3-dimethylaminopropyl)-N'-ethylcarbodiimide hydrochloride
EDTA	ethylenediaminetetraacetic acid
EFV	efavirenz
FBS	fetal bovine serum
HAART	highly active antiretroviral therapy
HEK	human embryonic kidney
HIV	human immunodeficiency virus
¹ H– ¹ H COSY	¹ H– ¹ H correlation spectroscopy
HMBC	heteronuclear multiple bond correlation
HPLC	high performance liquid chromatography
HRMS	high resolution mass spectrum
IN	integrase
IC ₅₀	half maximal inhibitory concentration
m-CPBA	3-chloroperbenzoic acid
NNRTI	non-nucleoside reverse transcriptase inhibitor
NVP	nevirapine
OD ₄₅₀	optical density at 450 nm
PBS	phosphate buffer saline
PR	protease
RAL	raltegravir
RT	reverse transcriptase
SAR	structure-activity relationship
TOA	time-of-drug addition

References

- [1] D.C. Douek, M. Roederer, R.A. Koup, Emerging concepts in the immunopathogenesis of AIDS, *Annu. Rev. Med.* 60 (2009) 471–484.
- [2] World Health Organization, July 18). HIV/AIDS, 2018. Retrieved from, <https://www.who.int/en/news-room/fact-sheets/detail/hiv-aids>.
- [3] United States Department of Health and Human Services, Global Statistics." *HIV.Gov*, 31 July 2019. www.hiv.gov/hiv-basics/overview/data-and-trends/global-statistics.
- [4] X. Zhang, Anti-retroviral drugs: current state and development in the next decade, *Acta Pharm. Sin.* B 8 (2018) 131–136.
- [5] J.M. Guo, M.Y. Ba, Y. Yang, C.S. Yao, M. Yu, J.G. Shi, Y. Guo, Discovery of a semi-synthesized cyclolignan as a potent HIV-1 non-nucleoside reverse transcriptase inhibitor, *J. Asian Nat. Prod. Res.* 21 (2017) 76–85.
- [6] A. Engelman, P. Cherepanov, The structural biology of HIV-1: mechanistic and therapeutic insights, *Nat. Rev. Microbiol.* 10 (2012) 279–290.
- [7] R.K. Gupta, J. Gregson, N. Parkin, H. Haile-Selassie, A. Tanuri, L. Andrade

- Forero, P. Kaleebu, C. Watera, A. Aghokeng, N. Mutenda, J. Dzangare, S. Hone, Z.Z. Hang, J. Garcia, Z. Garcia, P. Marchorro, E. Beteta, A. Giron, R. Hamers, S. Inzaule, L.M. Frenkel, M.H. Chung, T. de Oliveira, D. Pillay, K. Naidoo, A. Kharsany, R. Kugathasan, T. Cutino, G. Hunt, S. Avila Rios, M. Doherty, M.R. Jordan, S. Bertagnolio, HIV-1 drug resistance before initiation or re-initiation of first-line antiretroviral therapy in low-income and middle-income countries: a systematic review and meta-regression analysis, *Lancet Infect. Dis.* 18 (2018) 346–355.
- [8] J. Ren, D.K. Stammers, Structural basis for drug resistance mechanisms for non-nucleoside inhibitors of HIV reverse transcriptase, *Virus Res.* 134 (2008) 157–170.
- [9] V. Namasivayam, M. Vanangamudi, V.G. Kramer, S. Kurup, P. Zhan, X. Liu, J. Kongsted, S.N. Byrareddy, The journey of HIV-1 non-nucleoside reverse transcriptase inhibitors (NNRTIs) from lab to clinic, *J. Med. Chem.* 62 (2019) 4851–4883.
- [10] M.S.A. Gill, S.S. Hassan, N. Ahemad, Evolution of HIV-1 reverse transcriptase and integrase dual inhibitors: recent advances and developments, *Eur. J. Med. Chem.* 179 (2019) 423–448.
- [11] J. Tang, H.T. Do, A.D. Huber, M.C. Casey, K.A. Kirby, D.J. Wilson, J. Kankanala, M.A. Parniak, S.G. Sarafianos, Z. Wang, Pharmacophore-based design of novel 3-hydroxypyrimidine-2,4-dione subtypes as inhibitors of HIV reverse transcriptase-associated RNase H: tolerance of a nonflexible linker, *Eur. J. Med. Chem.* 166 (2019) 390–399.
- [12] Y. Sang, S. Han, C. Pannecouque, E. De Clercq, C. Zhuang, F. Chen, Ligand-based design of nondimethylphenyl-diarylpiperidines with improved metabolic stability, safety, and oral pharmacokinetic profiles, *J. Med. Chem.* 62 (2019) 11430–11436.
- [13] T. Xiao, J.F. Tang, G. Meng, C. Pannecouque, Y.Y. Zhu, G.Y. Liu, Z.Q. Xu, F.S. Wu, S.X. Gu, F.E. Chen, Indazolyl-substituted piperidin-4-yl-aminopyrimidines as HIV-1 NNRTIs: design, synthesis and biological activities, *Eur. J. Med. Chem.* (2019) 111864.
- [14] M. Zhu, L. Ma, J. Wen, B. Dong, Y. Wang, Z. Wang, J. Zhou, G. Zhang, J. Wang, Y. Guo, C. Liang, S. Cen, Y. Wang, Rational design and Structure-Activity relationship of coumarin derivatives effective on HIV-1 protease and partially on HIV-1 reverse transcriptase, *Eur. J. Med. Chem.* (2019) 111900.
- [15] S. Han, Y. Sang, Y. Wu, Y. Tao, C. Pannecouque, E. De Clercq, C. Zhuang, F.E. Chen, Fragment hopping-based discovery of novel sulfinylacetamide-diarylpiperidines (DAPYs) as HIV-1 nonnucleoside reverse transcriptase inhibitors, *Eur. J. Med. Chem.* 185 (2020) 111874.
- [16] E. Tramontano, A. Corona, L. Menendez-Arias, Ribonuclease H, an unexploited target for antiviral intervention against HIV and hepatitis B virus, *Antivir. Res.* 171 (2019) 104613.
- [17] Jiangsu New Medical College, Dictionary of Traditional Chinese Medicine, vol. 1, Shanghai Scientific and Technical Publishers, Shanghai, 1986, 126, 1250.
- [18] S.L. Hsuan, S.C. Chang, S.Y. Wang, T.L. Liao, T.T. Jong, M.S. Chien, W.C. Lee, S.S. Chen, J.W. Liao, The cytotoxicity to leukemia cells and antiviral effects of *Isatis indigotica* extracts on pseudorabies virus, *J. Ethnopharmacol.* 123 (2009) 61–67.
- [19] J. Liu, Z. Jiang, R. Wang, Y. Zheng, J. Chen, X. Zhang, Y. Ma, Isatisine A, a novel alkaloid with an unprecedented skeleton from Leaves of *Isatis indigotica*, *Org. Lett.* 9 (2007) 4127–4129.
- [20] M. Chen, L. Gan, S. Lin, X. Wang, L. Li, Y. Li, C. Zhu, Y. Wang, B. Jiang, J. Jiang, Y. Yang, J. Shi, Alkaloids from the root of *Isatis indigotica*, *J. Nat. Prod.* 75 (2012) 1167–1176.
- [21] M. Chen, S. Lin, L. Li, C. Zhu, X. Wang, Y. Wang, Enantiomers of an indole alkaloid containing unusual dihydrothiopyran and 1,2,4-thiadiazole rings from the root of *Isatis indigotica*, *Org. Lett.* 14 (2012) 5668–5671.
- [22] X. Wang, M. Chen, F. Wang, P. Bu, S. Lin, C. Zhu, Chemical constituents from root of *Isatis indigotica*, *China, J. Chin. Mater. Med.* 38 (2013) 1172–1182.
- [23] Y.-F. Liu, M.-H. Chen, X.-L. Wang, Q.-L. Guo, C.-G. Zhu, S. Lin, C.-B. Xu, Y.-P. Jiang, Y.-H. Li, J.-D. Jiang, Y. Li, J.-G. Shi, Antiviral enantiomers of a bisindole alkaloid with a new carbon skeleton from the roots of *Isatis indigotica*, *Chin. Chem. Lett.* 26 (2015) 931–936.
- [24] Y.F. Liu, M.H. Chen, Q.L. Guo, S. Lin, C.B. Xu, Y.P. Jiang, Y.H. Li, J.D. Jiang, J.G. Shi, Antiviral glycosidic bisindole alkaloids from the roots of *Isatis indigotica*, *J. Asian Nat. Prod. Res.* 17 (2015) 689–704.
- [25] Y.F. Liu, M.H. Chen, S. Lin, Y.H. Li, D. Zhang, J.D. Jiang, J.G. Shi, Indole alkaloid glycosides from the roots of *Isatis indigotica*, *J. Asian Nat. Prod. Res.* 18 (2016) 1–12.
- [26] Y. Liu, X. Wang, M. Chen, S. Lin, L. Li, J. Shi, Three pairs of alkaloid enantiomers from the root of *Isatis indigotica*, *Acta Pharm. Sin. B* 6 (2016) 141–147.
- [27] M.-H. Chen, S. Lin, Y.-N. Wang, C.-G. Zhu, Y.-H. Li, J.-D. Jiang, J.-G. Shi, Antiviral stereoisomers of 3,5-bis(2-hydroxybut-3-en-1-yl)-1,2,4-thiadiazole from the roots of *Isatis indigotica*, *Chin. Chem. Lett.* 27 (2016) 643–648.
- [28] Y. Liu, M. Chen, Q. Guo, Y. Li, J. Jiang, J. Shi, Aromatic compounds from an aqueous extract of "ban lan gen" and their antiviral activities, *Acta Pharm. Sin. B* 7 (2017) 179–184.
- [29] L. Meng, Q. Guo, Y. Liu, M. Chen, Y. Li, J. Jiang, J. Shi, Indole alkaloid sulfonic acids from an aqueous extract of *Isatis indigotica* roots and their antiviral activity, *Acta Pharm. Sin. B* 7 (2017) 334–341.
- [30] L.J. Meng, Q.L. Guo, C.B. Xu, C.G. Zhu, Y.F. Liu, M.H. Chen, S. Lin, Y.H. Li, J.D. Jiang, J.G. Shi, Diglycosidic indole alkaloid derivatives from an aqueous extract of *Isatis indigotica* roots, *J. Asian Nat. Prod. Res.* 19 (2017) 529–540.
- [31] L. Meng, Q. Guo, Y. Liu, J. Shi, 8,4'-Oxyneolignane glycosides from an aqueous extract of "ban lan gen" (*Isatis indigotica* root) and their absolute configurations, *Acta Pharm. Sin. B* 7 (2017) 638–646.
- [32] L.-J. Meng, Q.-L. Guo, C.-G. Zhu, C.-B. Xu, J.-G. Shi, Isatindigodiphindoside, an alkaloid glycoside with a new diphenylpropylindole skeleton from the root of *Isatis indigotica*, *Chin. Chem. Lett.* 29 (2018) 119–122.
- [33] L. Meng, Q. Guo, M. Chen, J. Jiang, Y. Li, J. Shi, Isatindolignanoside A, a glucosidic indole-lignan conjugate from an aqueous extract of the *Isatis indigotica* roots, *Chin. Chem. Lett.* 29 (2018) 1257–1260.
- [34] Q. Guo, C. Xu, M. Chen, S. Lin, Y. Li, C. Zhu, J. Jiang, Y. Yang, J. Shi, Sulfur-enriched alkaloids from the root of *Isatis indigotica*, *Acta Pharm. Sin. B* 8 (2018) 933–943.
- [35] M.A. Seyed, A comprehensive review on Phyllanthus derived natural products as potential chemotherapeutic and immunomodulators for a wide range of human diseases, *Biocatal. Agricult. Biotechnol.* 17 (2019) 529–537.
- [36] P. Habibi, H. Daniell, C.R. Soccol, M.F. Grossi-de-Sa, The potential of plant systems to break the HIV-TB link, *Plant Biotechnol. J* 17 (2019) 1868–1891.
- [37] C.C. Fernandes-Silva, A. Salatino, L.B. Barbosa-Motta, G. Negri, M.L.F. Salatino, Chemical characterization, antioxidant and anti-HIV activities of a Brazilian propolis from Ceará state, *Rev. Bras. Farmacogn.* 29 (2019) 309–318.
- [38] K.C. Chinsebu, Chemical diversity and activity profiles of HIV-1 reverse transcriptase inhibitors from plants, *Rev. Bras. Farmacogn.* 29 (2019) 504–528.
- [39] H.D. Zhao, Y. Lu, M. Yan, C.H. Chen, S.L. Morris-Natschke, K.H. Lee, D.F. Chen, Rapid recognition and targeted isolation of anti-HIV daphnane diterpenes from *Daphne genkwa* guided by UPLC-MSⁿ, *J. Nat. Prod.*, DOI: 10.1021/acs.jnatprod.9b00993.
- [40] V.P. Sonar, A. Corona, S. Distinto, E. Maccioni, R. Meleddu, B. Fois, C. Floris, N.V. Malpure, S. Alcaro, E. Tramontano, F. Cottiglia, Natural product-inspired esters and amides of ferulic and caffeic acid as dual inhibitors of HIV-1 reverse transcriptase, *Eur. J. Med. Chem.* 130 (2017) 248–260.
- [41] V. Pawar, D. Lokwani, S. Bhandari, D. Mitra, S. Sabde, K. Bothara, A. Madgulkar, Design of potential reverse transcriptase inhibitor containing Isatin nucleus using molecular modeling studies, *Bioorg. Med. Chem.* 18 (2010) 3198–3211.
- [42] V. Famigli, G. La Regina, A. Coluccia, S. Pelliccia, A. Brancale, G. Maga, E. Crespan, R. Badia, B. Clotet, J.A. Este, R. Cirilli, E. Novellino, R. Silvestri, New indolylarylsulfones as highly potent and broad spectrum HIV-1 non-nucleoside reverse transcriptase inhibitors, *Eur. J. Med. Chem.* 80 (2014) 101–111.
- [43] A. Corona, R. Meleddu, F. Esposito, S. Distinto, G. Bianco, T. Masaoka, E. Maccioni, L. Menendez-Arias, S. Alcaro, S.F. Le Grice, E. Tramontano, Ribonuclease H/DNA polymerase HIV-1 reverse transcriptase dual inhibitor: mechanistic studies on the allosteric mode of action of isatin-based compound RMNC6, *PLoS One* 11 (2016), e0147225.
- [44] X. Li, P. Gao, P. Zhan, X. Liu, Substituted indoles as HIV-1 non-nucleoside reverse transcriptase inhibitors: a patent evaluation (WO2015044928), *Expert Opin. Ther. Pat.* 26 (2016) 629–635.
- [45] C. Dousson, F.R. Alexandre, A. Amador, S. Bonaric, S. Bot, C. Caillet, T. Convard, D. da Costa, M.P. Lioure, A. Roland, E. Rosinovsky, S. Maldonado, C. Parsy, C. Trochet, R. Storer, A. Stewart, J. Wang, B.A. Mayes, C. Musiu, B. Poddesu, L. Vargiu, M. Liuzzi, A. Moussa, J. Jakubik, L. Hubbard, M. Seifer, D. Standing, Discovery of the Aryl-phospho-indole IDX899, a highly potent anti-HIV non-nucleoside reverse transcriptase inhibitor, *J. Med. Chem.* 59 (2016) 1891–1898.
- [46] S. Brigg, N. Pribut, A.E. Basson, M. Avgenikos, R. Venter, M.A. Blackie, W.A.L. van Otterlo, S.C. Pelly, Novel indole sulfides as potent HIV-1 NNRTIs, *Bioorg. Med. Chem. Lett.* 26 (2016) 1580–1584.
- [47] T.L. Devale, J. Parikh, P. Miniyar, P. Sharma, B. Shrivastava, P. Murumkar, Dihydropyrimidinone-isatin hybrids as novel non-nucleoside HIV-1 reverse transcriptase inhibitors, *Bioorg. Chem.* 70 (2017) 256–266.
- [48] R. Meleddu, S. Distinto, A. Corona, E. Tramontano, G. Bianco, C. Melis, F. Cottiglia, E. Maccioni, Isatin thiazoline hybrids as dual inhibitors of HIV-1 reverse transcriptase, *J. Enzym. Inhib. Med. Chem.* 32 (2017) 130–136.
- [49] C. Pu, R.H. Luo, M. Zhang, X. Hou, G. Yan, J. Luo, Y.T. Zheng, R. Li, Design, synthesis and biological evaluation of indole derivatives as Vif inhibitors, *Bioorg. Med. Chem. Lett.* 27 (2017) 4150–4155.
- [50] V. Famigli, G. La Regina, A. Coluccia, D. Masci, A. Brancale, R. Badia, E. Limeira-Munoz, J.A. Este, E. Crespan, A. Brambilla, G. Maga, M. Catalano, C. Limatola, F.R. Formica, R. Cirilli, E. Novellino, R. Silvestri, Chiral indolylarylsulfone non-nucleoside reverse transcriptase inhibitors as new potent and broad spectrum anti-HIV-1 Agents, *J. Med. Chem.* 60 (2017) 6528–6547.
- [51] X. Li, P. Gao, B. Huang, Z. Zhou, Z. Yu, Z. Yuan, H. Liu, C. Pannecouque, D. Daelemans, E. De Clercq, P. Zhan, X. Liu, Discovery of novel piperidine-substituted indolylarylsulfones as potent HIV NNRTIs via structure-guided scaffold morphing and fragment rearrangement, *Eur. J. Med. Chem.* 126 (2017) 190–201.
- [52] T. Zhao, Q. Meng, D. Kang, J. Ji, E. De Clercq, C. Pannecouque, X. Liu, P. Zhan, Discovery of novel indolylarylsulfones as potent HIV-1 NNRTIs via structure-guided scaffold morphing, *Eur. J. Med. Chem.* 182 (2019) 111619.
- [53] I. Hdoufane, J. Stoycheva, A. Tadjer, D. Villemain, M. Najdoska-Bogdanov, J. Bogdanov, D. Cherqaoui, QSAR and molecular docking studies of indole-based analogs as HIV-1 attachment inhibitors, *J. Mol. Struct.* 1193 (2019) 429–443.
- [54] S. Kumar, S. Gupta, L.F. Abadi, S. Gaikwad, D. Desai, K.K. Bhutani, S. Kulkarni, I.P. Singh, Synthesis and in-vitro anti-HIV-1 evaluation of novel pyrazolo[4,3-c]pyridin-4-one derivatives, *Eur. J. Med. Chem.* 183 (2019) 111714.
- [55] F. Esposito, M. Sechi, N. Pala, A. Sanna, P.C. Koneru, M. Kvaratskhelia, L. Naesens, A. Corona, N. Grandi, R. di Santo, V.M. D'Amore, F.S. Di Leva,

- E. Novellino, S. Cosconati, E. Tramontano, Discovery of dihydroxyindole-2-carboxylic acid derivatives as dual allosteric HIV-1 integrase and reverse transcriptase associated ribonuclease H inhibitors, *Antivir. Res.* 174 (2019) 104671.
- [56] Y. Cao, S. Li, H. Chen, Y. Guo, Establishment of pharmacological evaluation system for non-nucleoside reverse transcriptase inhibitors resistant HIV-1, *Acta Pharm. Sin.* 44 (2009) 355–361.
- [57] D.N. Kursanov, Z.N. Parnes, N.M. Loim, Applications of ionic hydrogenation to organic synthesis, *Synthesis* 9 (1974) 633–651.
- [58] M. Somei, T. Kawasaki, A new and simple synthesis of 1-hydroxyindole derivatives, *Heterocycles* 29 (1989) 1251–1254.
- [59] X. Ma, L. Li, T. Zhu, M. Ba, G. Li, Q. Gu, Y. Guo, D. Li, Phenylspirodrimanes with anti-HIV activity from the sponge-derived fungus *Stachybotrys chartarum* MXH-X73, *J. Nat. Prod.* 76 (2013) 2298–2306.
- [60] Y. Yang, Y. Cao, H. Liu, H. Yan, Y. Guo, F. Shizukaol, A new structural type inhibitor of HIV-1 reverse transcriptase RNase H, *Acta Pharm. Sin.* 47 (2012) 1011–1016.
- [61] T. Tomakinian, C. Kouklovsky, G. Vincent, Investigation of the synthesis of benzofuroindolines from N-Hydroxyindoles: an O-Arylation/[3,3]-sigmatropic rearrangement sequence, *Synlett* 26 (2015) 1269–1275.
- [62] J. Meng, D. Du, G. Xiong, W. Wang, Y. Wang, H. Koshima, T. Matsuura, A dual pathway in the solid-state photoreaction of nitrobenzaldehydes with indole, *J. Heterocycl. Chem.* 31 (1994) 121–124.
- [63] M. Hu, C. Xu, C. Yang, H. Zuo, C. Chen, D. Zhang, G. Shi, W. Wang, J. Shi, T. Zhang, Discovery and evaluation of ZT55, a novel highly-selective tyrosine kinase inhibitor of JAK2(V617F) against myeloproliferative neoplasms, *J. Exp. Clin. Cancer Res.* 38 (2019) 49.
- [64] S.G. Sarafianos, B. Marchand, K. Das, D.M. Himmel, M.A. Parniak, S.H. Hughes, E. Arnold, Structure and function of HIV-1 reverse transcriptase: molecular mechanisms of polymerization and inhibition, *J. Mol. Biol.* 385 (2009) 693–713.
- [65] M. Figiel, M. Krepl, J. Poznanski, A. Golab, J. Sponer, M. Nowotny, Coordination between the polymerase and RNase H activity of HIV-1 reverse transcriptase, *Nucleic Acids Res.* 45 (2017) 3341–3352.
- [66] L. Tian, M.S. Kim, H. Li, J. Wang, W. Yang, Structure of HIV-1 reverse transcriptase cleaving RNA in an RNA/DNA hybrid, *Proc. Natl. Acad. Sci. U. S. A.* 115 (2018) 507–512.
- [67] Stanford University, Non-nucleoside RT inhibitor (NNRTI)-resistance mutations, Stanford HIV Drug-Resistance Database. <https://hivdb.stanford.edu/pages/3DStructures/rt.html#R>.
- [68] Y. Hsiou, J. Ding, K. Das, A.D. Clark Jr., P.L. Boyer, P. Lewi, P.A. Janssen, J.P. Kleim, M. Rosner, S.H. Hughes, E. Arnold, The Lys103Asn mutation of HIV-1 RT: a novel mechanism of drug resistance, *J. Mol. Biol.* 309 (2001) 437–445.
- [69] A.L. Hopkins, J. Ren, J. Milton, R.J. Hazen, J.H. Chan, D.I. Stuart, D.K. Stammers, Design of non-nucleoside inhibitors of HIV-1 reverse transcriptase with improved drug resistance properties. 1, *J. Med. Chem.* 47 (2004) 5912–5922.
- [70] J. Ren, C. Nichols, L. Bird, P. Chamberlain, K. Weaver, S. Short, D.I. Stuart, D.K. Stammers, Structural mechanisms of drug resistance for mutations at codons 181 and 188 in HIV-1 reverse transcriptase and the improved resilience of second generation non-nucleoside inhibitors, *J. Mol. Biol.* 312 (2001) 795–805.
- [71] A.H. Chan, W.G. Lee, K.A. Spasov, J.A. Cisneros, S.N. Kudalkar, Z.O. Petrova, A.B. Buckingham, K.S. Anderson, W.L. Jorgensen, Covalent inhibitors for eradication of drug-resistant HIV-1 reverse transcriptase: from design to protein crystallography, *Proc. Natl. Acad. Sci. U. S. A.* 114 (2017) 9725–9730.
- [72] K. Das, J.D. Bauman, A.D. Clark Jr., Y.V. Frenkel, P.J. Lewi, A.J. Shatkin, S.H. Hughes, E. Arnold, High-resolution structures of HIV-1 reverse transcriptase/TMC278 complexes: strategic flexibility explains potency against resistance mutations, *Proc. Natl. Acad. Sci. U.S.A.* 105 (2008) 1466–1471.
- [73] S.K. Ghosh, R. Nagarajan, Total synthesis of cruciferane via epoxidation/tandem cyclization sequence, *RSC Adv.* 4 (2014) 63147–63149.
- [74] X. Zhang, F. Yan, K. Tang, Q. Chen, J. Guo, W. Zhu, S. He, L. Banadyga, X. Qiu, Y. Guo, Identification of a clinical compound losmapimod that blocks Lassa virus entry, *Antivir. Res.* 167 (2019) 68–77.
- [75] D. Zhang, J. Guo, M. Zhang, X. Liu, M. Ba, X. Tao, L. Yu, Y. Guo, J. Dai, Oxazole-containing diterpenoids from cell cultures of *Salvia miltiorrhiza* and their anti-HIV-1 activities, *J. Nat. Prod.* 80 (2017) 3241–3246.